

**Optical and structural studies of samarium doped
strontium magneto silicate phosphor synthesized via
Sol-gel method**

A PROJECT REPORT

SUBMITTED TOWARDS THE PARTIAL FULFILLMENT OF THE
REQUIREMENTS FOR THE AWARD OF THE DEGREE
OF

MASTER OF SCIENCE
IN
PHYSICS

Submitted by:

RAJAT KATIYAR
(2K21/MSCPHY/61)

Under the supervision

of

Prof. A. S. Rao



Department of Applied Physics

DELHI TECHNOLOGICAL UNIVERSITY
(Formerly Delhi College of Engineering) Bawana Road, Delhi-110042

May 2023

DELHI TECHNOLOGICAL UNIVERSITY
(Formerly Delhi College of Engineering)
Bawana Road, Delhi - 110042

CANDIDATE'S DECLARATION

I hereby certify that the work which is presented in the Major Project – II entitled “**Optical and structural studies of samarium doped strontium magneto silicate phosphor synthesized via Sol-gel method**” in fulfillment of the requirement for the award of the Master of Science in Physics and submitted to the Department of Applied Physics, Delhi Technological University, Delhi is an authentic record of my own, carried out during the period from January to May 2023 under the supervision of Prof. A. S. Rao.

The matter presented in this report has not been submitted by me for the award of any other degree of this or any other Institute/University. The work has been communicated in peer reviewed Scopus indexed conference with the following details:

Title of the Paper: Optical and structural studies of samarium doped strontium magneto silicate phosphor synthesized via Sol-gel method

Author names: Rajat Katiyar, A.S. Rao

Name of Conference: International Conference on Thin Films & Nanotechnology: Knowledge, Leadership, & Commercialization

Conference Dates with venue: 6-8th July ; IIT Madras, Chennai

Conference Registered (Yes/No)? : Yes

Status of paper (Accepted/Published/Communicated):

Date of Paper Publication: Yet to be Published

Rajat Katiyar
2K21/MSCPHY/61

SUPERVISOR CERTIFICATE

To the best of my knowledge, the above work has not been submitted in part or full for any Degree or Diploma to this University or elsewhere. I, further certify that the publication and indexing information given by the students is correct.

Place:

Date:

Prof. A. S. Rao

ABSTRACT

Sol-gel synthesis method was used to synthesize a series of samarium ion doped strontium magneto silicate phosphors. The structural properties of strontium magneto silicate were characterized by X-ray Diffraction (XRD) method. Fourier Transform Infrared (FT-IR) reveals the presence of functional groups in the synthesized phosphor. Diffuse reflectance spectrum is reflecting the 4.39 eV optical band gap of undoped strontium magneto silicate phosphor. Under 404 nm excitation, luminescent spectra show it have distinctive emission peaks, owing to the transition of ${}^4G_{5/2} = {}^6H_J$ ($J = 5/2, 7/2, 9/2,$ and $11/2$) corresponding to the peaks centered at 564 nm, 601 nm, 646 nm and 708nm. Photoluminescence (PL) spectra shows that 2.0 mol % is the optimum concentration of Sm^{3+} ion to give the most intense reddish orange emission. The PL analysis shows that the exchange coupling interaction is responsible for the concentration quenching observed beyond 2.0 mol% of Sm^{3+} ions concentration. The chromaticity coordinates ($x=0.592$ and $y=0.406$) were calculated by photoluminescence spectra of optimized phosphor samples. The direct energy band gap was found to be 4.39 eV. All the investigation specified above signifies that the synthesized phosphor is well suited as a red emitter in lighting and display devices.

DELHI TECHNOLOGICAL UNIVERSITY
(Formerly Delhi College of Engineering)

Bawana Road, Delhi - 110042

ACKNOWLEDGEMENT

I would like to express my sincere gratitude to my guide and mentor, Prof. A. S. Rao, for guiding and assisting me in every step of this project. I am extremely grateful to him for giving me clear direction and moral support to carry out the project. I appreciate the continual assistance and convenience provided by all lab members (Ph.D. scholars), especially Mr. Videsh Kumar, Dept. of Applied Physics, at every stage of my study.

I am expressing my gratitude to the Department of Applied Physics for providing me with the required labs, infrastructure and environment which permitted me to perform my task without any hindrance.

Rajat Katiyar

TABLE OF CONTENTS

CANDIDATE'S DECLARATION	ii
SUPERVISOR CERTIFICATE	ii
ABSTRACT	iii
ACKNOWLEDGEMENT	iv
TABLE OF CONTENTS	v
LIST OF TABLES AND FIGURES	vii
LIST OF ABBREVIATIONS	viii
CHAPTER 1: INTRODUCTION	1
1.1 Phosphor	2
1.2 Host and activator ions	4
1.3 White light emitting diodes (w-LEDs)	5
1.4 Photoluminescence (PL)	7
CHAPTER 2: INSTRUMENTATION	11
2.1 X-ray diffraction (XRD)	12
2.2 Diffuse reflectance spectroscopy (DRS)	14
2.3 Fourier infrared transform spectroscopy (FT-IR)	15
2.4 Scanning electron microscope (SEM)	16
2.5 Photoluminescence (PL) spectroscopy	18
2.6 Decay time	19
CHAPTER 3: EXPERIMENTAL PROCEDURE	21
3.1 Synthesis: Sol Gel method	22
3.2 Sample preparation: SrMgSi ₂ O ₆	22
3.3 Analysis of sample	23
CHAPTER 4: RESULTS AND DISCUSSION	24
4.1 Structural studies	25
4.2 Diffuse Reflectance Spectroscopy	25
4.3 Fourier transform infrared spectroscopy	27
4.4 Morphological studies	29
4.5 Photoluminescence spectra	30
4.5.1 Excitation spectra	30
4.5.2 Emission spectra	31
4.6 Temperature Dependent Photoluminescence	33

4.7 Color chromaticity diagram for SMSS	35
CHAPTER 5: CONCLUSIONS	36
CHAPTER 6: SCOPE OF WORK	38
REFERENCES	40
PLAGIARISM REPORT	47
Abstract acceptance mail	48
REGISTRATION PROOF	49
PROOF OF SCOPUS INDEXING	50

LIST OF TABLES AND FIGURES

Fig. 1.1. Phosphor emitting Light

Fig. 1.2. Jablonski diagram showing various processes involved in PL

Fig. 2.1. Apparatus for X-ray Diffraction

Fig. 2.2. Schematic representation of Bragg's law

Fig. 2.3. Fourier infrared transform spectroscopy

Fig. 2.4. Apparatus for SEM

Fig. 4.1. XRD patterns of SMSS phosphor at different concentration of Sm³⁺ doped SMSS phosphor

Fig. 4.2. UV diffuse reflectance spectra of undoped and Sm³⁺ doped SMSS phosphor

Fig. 4.3. Energy band gap of 2.0 mol% Sm³⁺ doped SMSS phosphor

Fig. 4.4. FT-IR patterns of 2.0 mol% Sm³⁺ doped SMSS phosphor

Fig. 4.5. SEM micrographs of SMSS Phosphor

Fig. 4.6. PLE spectrum of Sm³⁺ doped SMSS phosphor at 601 nm emission wavelength

Fig. 4.7. Emission spectra of Sm³⁺ doped SMSS phosphor at 404 nm excitation wavelength

Fig. 4.8. Temperature dependent photoluminescence of 2.0 mol% Sm³⁺ doped SMSS phosphor at 404 nm excitation wavelength

Fig. 4.9. Plot for Activation Energy

Fig. 4.10. CIE chromaticity diagram of 2.0 mol% of Sm³⁺ doped SMSS phosphor under excitation wavelengths of $\lambda_{ex}=404$ nm

LIST OF ABBREVIATIONS

SMSS	-	Strontium Magneto Silicate
LED	-	Light-emitting diode
w-LED	-	White Light Emitting Diode
RE	-	Rare Earth (Metals)
CCT	-	Correlated Color Temperature
JCPDS	-	Joint Committee on Powder Diffraction Standards
SEM	-	Scanning Electron Microscope
CIE	-	Commission International De L' Eclairage
UV	-	Ultraviolet
PL	-	Photoluminescence
PLE	-	Photoluminescence Excitation
XRD	-	X-ray Diffraction
Vis	-	Visible

CHAPTER 1:

INTRODUCTION

1.1 Phosphor

Since the 19th century, phosphors have played a significant role in the field of luminous materials, capturing our attention with their ability to emit light when activated. These extraordinary materials have been used in a variety of devices, including fluorescent lights, workstation monitors, and video displays. Utilizing the potential of phosphors for various technological breakthroughs requires a thorough understanding of their intricate nature and distinctive traits.[1]

Inorganic substances can be generically categorized as phosphors, with dry powder being the most prevalent form. These powders are made up of a variety of different substances, such as oxides, oxynitrides, sulfides, selenides, halides, borates, and oxyhalides. The little numbers of activator ions that are introduced into the host matrix, however, are what really distinguish phosphors from other compounds. The rare-earth ions among these activator ions have proven to be particularly adaptable and are frequently used because of their positive interaction with the host material's crystalline lattice.

A key factor in phosphors' luminous behavior is their energy dynamics. Phosphors can take in energy at the activator ion level or at other locations within the lattice structure when subjected to excitation energy. The absorbed energy must eventually be transported to the radiating core, where light emission takes place, for luminescence to take place. Energy is efficiently captured and transferred by effective phosphors, who also maximize their quantum efficiency and reduce energy loss through non-radiative paths.



Fig. 1.1. Phosphor emitting Light

In many applications, the phosphors' emission characteristics are crucial. The wide spectrum of colors that a phosphor may display, including red, green, and blue, is one important characteristic. The creation of high-quality displays and lighting systems depends on the capacity to produce vivid and varied colors. To achieve precise color reproduction, the emission spectrum—which depicts the frequency distribution of the electromagnetic radiation—is meticulously crafted. Precise color points can be attained by using methods like the Commission International de L'Eclairage (CIE) graphic rule to compute the emission spectrum energy division.[2]

When considering phosphors for real-world applications, luminance and lumen equivalency are crucial considerations. Higher numbers denote a more intense light output, and luminosity relates to the perceived brightness of a light source. Lumen equivalence, on the other hand, gauges how effectively a phosphor produces visible light from absorbed energy. Per unit of input energy, a phosphor with a higher lumen equivalence generates more visible light. For applications that demand powerful, bright light sources, achieving high brightness and lumen equivalence is crucial.

The lifespan of their emission is another important factor for phosphor materials. Phosphors are economically feasible for a variety of applications because they have a long emission lifespan, which guarantees continuous and durable illumination. Phosphors must be able to endure prolonged use without significantly losing their emission intensity or color quality. This longevity is especially important for applications that call for continuous or prolonged lighting.

The fundamental characteristic of a phosphor's capacity to emit photons in response to incident triggering photons at particular wavelengths is known as quantum efficiency. By quantifying the energy conversion process' efficiency within the phosphor, it makes it possible to assess how well it performs. Quantum efficiency offers important insights into the overall efficiency of a phosphor in converting energy into light by measuring the quantity and wavelengths of emitted photons in relation to the number of incident photons.[3]

Phosphors' suitability for particular applications must be determined when they are synthesized, taking into account a number of factors. To make sure that phosphors can withstand the operating conditions of the intended device or system, chemical and thermal stability is essential. Additionally, in today's sustainable landscape, phosphors' environmental impact and biodegradability are important factors to take into account.

Furthermore, it would be ideal to be able to precisely control and engineer the emission characteristics of phosphors. To improve the performance and adaptability of phosphor

materials, research is still being done on adjusting the emission spectrum, improving quantum efficiency, and lengthening the emission lifetime. The characteristics of phosphors are continuously being improved thanks to improvements in synthesis methods like the controlled doping of activator ions and the creation of new composite materials.[4]

Phosphor materials have found use in many different industries, including thermal sensors, light-emitting diodes (LEDs), solar cells, plasma and field-emission displays, and many others. Their capacity to transform energy into light has revolutionized the lighting sector and made it possible to create lighting solutions that are both energy-efficient and environmentally friendly.[5] Phosphors are still at the forefront of research and development, fostering creativity and advancing a wide range of technologies.

In conclusion, phosphors are an intriguing class of luminescent materials that have influenced the development of our contemporary society. Phosphors have developed into an essential component in a variety of applications, from display technologies to energy-efficient lighting systems, through careful engineering and manipulation of their properties. Phosphors continue to open up new possibilities in a variety of fields, paving the way for brighter, more effective, and environmentally conscious technologies by improving their emission properties, improving quantum efficiency, extending emission lifespans, and taking environmental sustainability into account.

1.2 Host and activator ions

Phosphors, which consist of an activator and a host matrix, are essential for a wide range of technological applications, including lighting, displays, sensors, and fluorescence instruments. The development of phosphors has undergone a revolution thanks to the special qualities of rare earth dopants and hosts, which have improved performance and efficiency.

Due to their physical, thermal, and chemical inertness, inorganic hosts are frequently used in phosphors, making them excellent candidates for a variety of applications. However, self-activated hosts have attracted a lot of attention lately. These hosts don't require additional activators because they naturally produce intense, broad-spectrum visible radiation. Self-activated hosts are used, which improves emission intensity and streamlines phosphor synthesis procedures.

When stimulated, the activator, a dopant added to the phosphor material's crystal structure, causes light to emit. Because of their distinctive electronic structure and effective light emission characteristics, rare earth elements have become essential activator ions. Europium (Eu^{3+}), samarium (Sm^{3+}), and dysprosium (Dy^{3+}) are particularly significant rare earth dopants.[6]

The red luminescence of europium, which is frequently used as an activator ion, is

astounding. When compared to regular phosphors, rare earth (Eu^{3+}) phosphors increase brightness in liquid crystal display (LCD) panels by a factor of ten. Displays that are brighter and more visually appealing as a result of this extraordinary brightness improvement. Additionally, compared to conventional incandescent lights, white LEDs using a combination of three rare earth phosphors, including europium, show a remarkable 80% increase in energy efficiency. The development of superior energy-saving lighting solutions has been made possible by the inclusion of rare earth elements in phosphor formulations.

Samarium-doped phosphors have drawn a lot of interest because of their diverse emission characteristics. Samarium ions' transition from $^4\text{G}_{5/2}$ to $^6\text{H}_J$ is especially useful for a variety of applications. Samarium-doped phosphors aid high-density sensors in optical storage by enabling optical retention and accurate data retrieval.[7] Samarium phosphors are also used in underwater communication systems to take advantage of their distinct emission properties. The emission characteristics of samarium ions are used in fluorescent devices and color displays to produce vivid and accurate color representation.

Another prominent rare earth dopant called dysprosium is essential for creating effective, high-performance phosphors. Dysprosium-doped phosphors are especially well suited for applications that demand persistent emission of light due to their distinctive emission characteristics and long luminescent lifetimes.[8] This characteristic is useful in plasma displays and cathode ray tubes (CRTs), where phosphors with long persistence are used to produce persistent afterglow for better image quality and less flicker.

The selection of the host material is equally important as the rare earth dopants, which offer exceptional luminescent properties. Trivalent rare earth ions doped in borates, such as Sm^{3+} , Dy^{3+} , and Eu^{3+} , have attracted a lot of attention lately. Outstanding stability, broad UV transparency, low composite temperature, and high luminous efficiency are all features of hosts made of borate. Borates are useful in a variety of optical applications because they also have a wide transmittance spectrum. The exceptional optical quality and high thermal stability of the borate hosts contribute to the phosphor's overall performance and longevity.[9]

To sum up, the development of phosphors has been revolutionized by rare earth dopants and hosts, which offer exceptional luminescent qualities and enhanced performance. Activator ions made from rare earth elements like dysprosium, europium, and samarium improve brightness, energy efficiency, and color representation in a variety of applications. Stability, transparency, and high luminous efficiency are ensured by choosing the right host materials, such as borates. Rare earth dopants and hosts will continue to drive innovation in lighting, displays, sensors, and fluorescence instruments as phosphor research develops, providing remarkable solutions for a variety of technological needs.

1.3 White light emitting diodes (w-LEDs)

The lighting industry has undergone a revolution thanks to the superior efficiency, long lifespan, and versatility of white light-emitting diodes (LEDs). Initially, individual red,

green, and blue LEDs were combined in a single package to produce white LEDs. However, improvements in phosphor technology have paved the way for white LEDs that are more effective and of higher quality.

Phosphors are essential to LEDs' ability to produce white light. They are substances with the capacity to absorb light at one wavelength and reemit it at another. When it comes to white LEDs, phosphors are used to change the blue light emitted by the blue LED chip into yellow light, which when combined with the blue light being transmitted, produces white light.[10]

Traditionally, the encapsulation of the LED package was coated with a mixture of phosphors to create white LEDs. The phosphors produced a wide spectrum of white light by absorbing some of the blue light and emitting yellow light. However, this strategy had drawbacks, including light reabsorption by the phosphors and decreased luminous performance as a result of the red and green phosphors' poor performance in particular wavelength ranges.

Researchers have used rare earth elements as dopants in phosphors to get around these problems. These elements are perfect for use in phosphor-converted LEDs because they have impressive photoluminescence properties in a variety of compounds. In addition to having a low color temperature and a high color rendering index (CRI), rare earth-doped phosphors have a number of benefits. The LEDs are perfect for applications where color fidelity is important because the low color temperature ensures that the light they emit has a warm tone, similar to that of conventional incandescent bulbs, and the high CRI shows that they can render colors accurately.

Utilizing tri-color phosphors that are activated by near-UV light is one innovative advancement in white LED technology. This novel method makes use of phosphors that react to UV light between 370 and 410 nm.[11] The tri-color phosphors can effectively convert UV light into a wide spectrum of visible light, producing a full spectrum of white light by incorporating near-UV LEDs into the LED package. This method has benefits like improved color rendering capabilities, enhanced tolerance to UV chip color variations, and consistent white light production.

Phosphors have other advantageous qualities in addition to their optical properties. They have a high efficiency, which effectively transforms absorbed energy into light, increasing the white LED's energy efficiency. Furthermore, phosphors have a low dissipation potential, enabling better thermal control inside the LED package. Because of this characteristic, white LEDs have a long lifespan and maintain their performance for a long time.[12]

The relatively low toxicity of phosphors is another noteworthy benefit. White LEDs based on phosphor are more environmentally friendly than conventional lighting technologies, which use potentially dangerous materials like mercury in fluorescent lamps. When their lifespan is up, they can be safely disposed of with little risk to human health.

Phosphor-doped white LEDs are a significant improvement in lighting technology, to sum up. These LEDs produce high-quality, full-spectrum white light, which enhances their capacity for color rendering, energy efficiency, and lifespan. The performance and efficiency of white LEDs have been further enhanced by the use of rare earth-doped phosphors and the development of tri-color phosphors that are near-UV activated. Phosphor-doped white LEDs are poised to play a crucial role in illuminating our future with sustainable and brilliant lighting solutions as the demand for energy-efficient lighting keeps rising.

1.4 Photoluminescence (PL)

The study of materials and their optical properties is greatly aided by the fascinating phenomenon of photoluminescence. When a substance absorbs photons, a process known as photoluminescence may occur in which it emits light after being exposed to light. The electronic composition and energy levels of the material can be learned a lot from this light emission. Understanding fluorescence and phosphorescence, two particular forms of photoluminescence, is crucial for digging deeper into the subject. The Jablonski diagram is also a helpful tool for understanding and visualizing the energy transitions connected to photoluminescence.

A characteristic of the photoluminescent process known as fluorescence is the instantaneous emission of light upon photon absorption. This process involves the excitation of a material's electrons from their ground state to higher energy levels when it absorbs photons. However, through a process known as fluorescence, the excited electrons quickly return to a lower energy level rather than relaxing back to the ground state. The emission of a photon with a longer wavelength, usually in the visible or ultraviolet range, occurs simultaneously with this rapid relaxation. Fluorescence happens in a matter of nanoseconds or less, on average. Fluorescence is useful in a variety of applications, such as biological imaging, chemical sensing, and fluorescent lighting, due to its quick emission process.

On the other hand, phosphorescence is an additional variety of photoluminescence that involves a delayed emission of light following photon absorption. In contrast to fluorescence, phosphorescence involves an extremely gradual return of excited electrons to their ground state. Depending on the particular material, this delay can last anything

from a few nanoseconds to several hours. The excited electrons may go through additional intersystem crossing (ISC) processes during this transition, changing their spin state prior to emitting a photon. Glow-in-the-dark materials, phosphor screens, and organic light-emitting diodes (OLEDs) all use the longer energy storage and release times of phosphorescent materials to their advantage.

The Jablonski diagram offers a useful framework for comprehending the fluorescence and phosphorescence processes. The energy levels and transitions that take place during photoluminescence are depicted in the Jablonski diagram. The ground state is at the bottom and higher energy levels are shown above it in a series of horizontal lines that represent different energy levels.

An electron is promoted from its ground state to an excited state by the material's absorption of a photon, which is the first step in the Jablonski diagram. The upward arrow pointing from the ground state to the excited state, which signifies this process as absorption, connects the two states. As determined by the wavelength of the incident light, the energy difference between these states corresponds to the energy of the absorbed photon.[13]

The excited electron has a variety of relaxation processes it can go through after absorption. The energy is released as heat through collisions with nearby atoms or molecules in the first relaxation pathway, known as vibrational relaxation. The electron is quickly brought to the lowest vibrational level possible while still in the excited state through a process called vibrational relaxation.

Internal conversion (IC) and intersystem crossing (ISC) are the two main ways that the electron can relax from the excited vibrational level. The excited electron transitions non-radiatively to a lower electronic energy level while maintaining the same spin state. An arrow connecting the excited state to a lower energy level within the same electronic state in a diagonal downward direction symbolizes this process.

The excited electron changes its spin state during intersystem crossing, which is a spin-forbidden transition. This transition takes place between states with varying levels of multiplicity, usually between singlet and triplet states. The excited state and a lower energy level of a different spin state are crossed by a curved arrow to signify intersystem crossing.

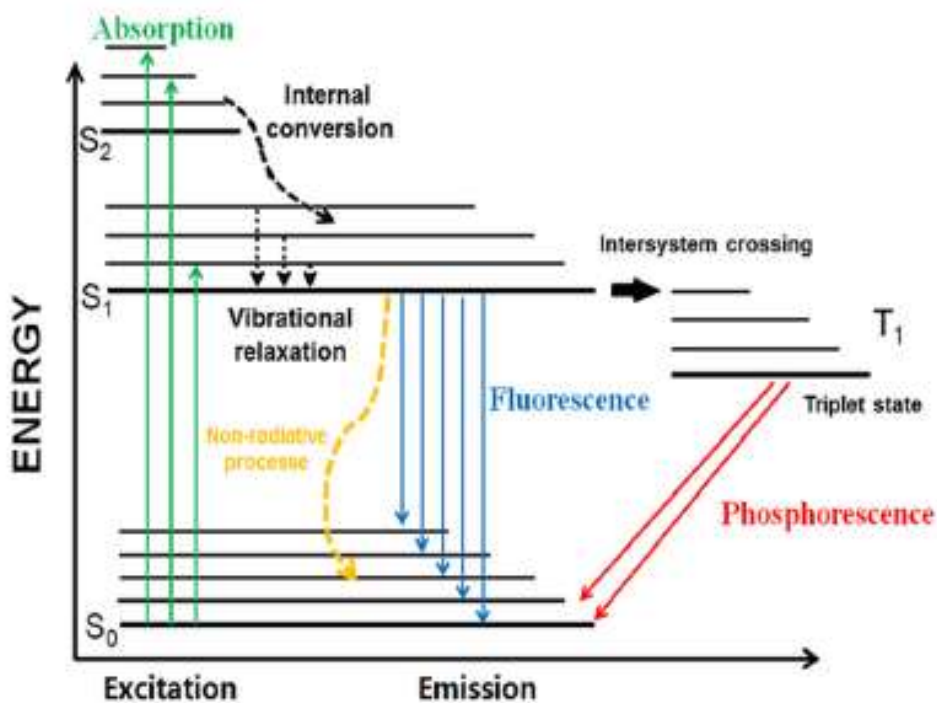


Fig. 1.2. Jablonski diagram showing various processes involved in PL

The electron enters a long-lived excited state after internal conversion or intersystem crossing, which is frequently referred to as a metastable state. In fluorescence, a photon is released through fluorescence emission as the excited electron quickly relaxes back to the ground state. The metastable state and ground state are connected by a downward arrow in this emission process, with the emitted photon carrying less energy than the absorbed photon.

In the case of phosphorescence, the electron experiences additional spin-flip processes after reaching the metastable state before going back to the ground state. These procedures involve the spin of the electron being reversed, which causes a delay in the photon's emission. A longer arrow from the metastable state to the ground state, signifying the longer timescale involved in this process, represents the phosphorescence emission.[14]

The energy transitions involved in photoluminescence, such as absorption, vibrational relaxation, internal conversion, intersystem crossing, and fluorescence or phosphorescence emission, are all depicted in detail in the Jablonski diagram. This illustration is a useful tool for comprehending photoluminescent material dynamics and creating applications that take advantage of their special characteristics.

In conclusion, photoluminescence is a potent method for learning about the optical

characteristics of materials. Two different types of photoluminescence, phosphorescence and fluorescence, are distinguished by the immediate and delayed emission of light, respectively. The Jablonski diagram sheds light on the underlying mechanisms by illuminating the various energy transitions that take place during photoluminescence. These ideas will enable researchers to delve deeper into the fascinating world of photoluminescence and its many applications, from materials science to biological imaging and beyond.

CHAPTER 2:

INSTRUMENTATION

2.1 X-ray diffraction (XRD)

An effective and frequently used method for examining the atomic and molecular structure of materials is X-ray diffraction (XRD). It involves the scattering of X-ray photons by the atoms within a crystal lattice, producing a distinctive diffraction pattern that can reveal important details about the structure and characteristics of the material.



Fig. 2.1. Apparatus for X-ray Diffraction

Bragg's law, which outlines the prerequisites for constructive interference of the scattered X-rays, is one of the fundamental tenets of XRD.

According to Bragg's law, two X-ray waves will constructively interfere and produce a strong diffraction peak if their paths are separated by an integer multiple of the X-ray wavelength and are scattered from adjacent crystal lattice planes.

This can be mathematically represented as:

$$n\lambda = 2d \sin(\theta) \quad (1)$$

In this equation, n stands for the order of diffraction, d for the distance between crystal lattice planes, θ for the angle between the incident X-ray beam and the normal to the lattice planes, and λ for the wavelength of the incident X-rays. With the help of Bragg's law, we can calculate the crystal lattice's interplanar spacing (d) from the observed diffraction angle (θ) and the known X-ray wavelength (λ). [15]

Obtaining a diffraction pattern, which is typically captured using a diffractometer, is

necessary for the analysis of XRD data. This device rotates the sample while calculating the intensity of the X-rays that are diffracted at various angles. The scattering from various crystallographic planes in the material is represented by a series of peaks in the resulting diffraction pattern.

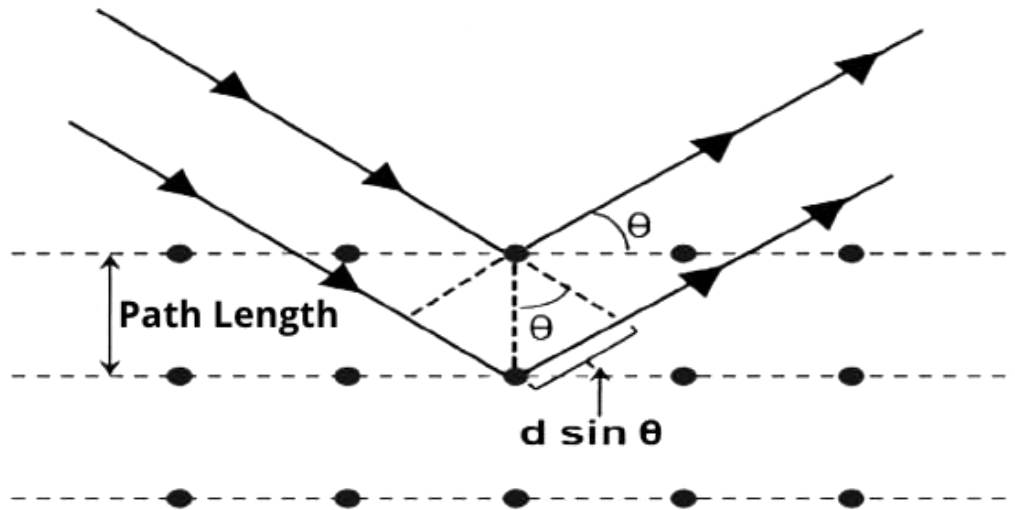


Fig. 2.2. Schematic representation of Bragg's law

The observed diffraction pattern is contrasted with known patterns kept in databases like the Powder Diffraction File (PDF) in order to identify and characterize a material using XRD. By comparing the observed peaks with the reference patterns, these databases, which contain the diffraction patterns of numerous materials, enable the identification of unidentified substances. The crystal structure, lattice parameters, and orientation of the substance can all be inferred from the position, intensity, and shape of the diffraction peaks.

Numerous types of information about a material can be obtained from XRD analysis. The crystal structure, including the sizes of the unit cells and the configuration of the atoms within the lattice, can be ascertained from the positions and intensities of the diffraction peaks. Peak widths can reveal information about the material's microstrain, defects, and dislocations, as well as the size of the crystallites. Peak shapes and intensities can be examined to learn more about the preferred crystal orientations and texture.

Additionally, phase identification with XRD enables the identification of the various crystallographic phases present in a sample. It is possible to identify various crystalline phases and determine their relative proportions by examining the relative intensities and positions of the diffraction peaks.[16]

The presence of preferred crystallographic orientations, residual stress, and other physical

properties can all be determined by XRD in addition to structural analysis. It is possible to obtain quantitative data about these properties by carefully examining the size and placement of the diffraction peaks, which can be essential for comprehending the behavior and performance of materials.

The capabilities and accuracy of XRD technology have recently been improved thanks to developments like the creation of high-resolution detectors and sophisticated data analysis methods. Additionally, new opportunities for automating and optimizing the analysis of XRD data have emerged, enabling quicker and more precise characterization of materials. This is made possible by the integration of artificial intelligence and machine learning approaches.

In conclusion, X-ray diffraction is a flexible and effective method for examining the structure and characteristics of materials. The diffraction phenomenon can be understood fundamentally thanks to Bragg's law, which also makes it possible to calculate interplanar spacings and gather crystallographic data. Crystal structure, phase identification, crystallite size, texture, residual stress, and other physical properties can all be learned from the diffraction pattern using XRD. The effectiveness and precision of the technique are being further improved by ongoing developments in XRD technology and the incorporation of AI tools, making it a vital tool in numerous scientific and industrial fields.

2.2 Diffuse reflectance spectroscopy (DRS)

A potent analytical method used to examine the optical characteristics of solid materials in the ultraviolet (UV) and visible (Vis) regions of the electromagnetic spectrum is UV-Visible Diffuse Reflectance Spectroscopy (UV-Vis DRS). UV-Vis DRS is particularly well suited for examining impenetrable solids, powders, and rough surfaces because it does not require the sample to be transparent or thin, unlike traditional transmission spectroscopy.

In UV-Vis DRS, light is emitted from a broad-spectrum light source that is typically a xenon lamp and is directed onto the sample surface. Due to the material's microscopic irregularities, the incident light interacts with it and diffuses reflection results. This indicates that the light is dispersed evenly rather than reflecting at particular angles (specular reflection).[17]

The reflected light is collected by a spectrophotometer with a diffuse reflectance accessory, which then measures the intensity of the light over a spectrum of wavelengths. The spectrum that was obtained, also referred to as the diffuse reflectance spectrum, offers important details about the sample's absorption and reflection characteristics. Researchers

can learn more about the electronic transitions, energy band gaps, and optical properties of a material by examining its spectral features, like the location and strength of its absorption bands or its reflectance minima and maxima.

UV-Vis DRS is used in a variety of industries. It is frequently employed in the characterization of semiconductors, minerals, pigments, and catalysts. The method enables the analysis of structural and electronic changes in materials, the identification of chemical species, and the quantification of constituents. In addition, UV-Vis DRS is employed in a variety of processes, including quality control, forensic science, and environmental analysis.[18]

Being non-destructive, requiring little sample preparation, and being able to analyze opaque or irregular samples are all benefits of UV-Vis DRS. It is a useful tool for materials characterization, research, and industrial analysis due to its adaptability and broad applicability.

2.3 Fourier infrared transform spectroscopy (FT-IR)

The interaction between infrared light and matter is studied using the highly adaptable and popular analytical technique known as Fourier Transform Infrared Spectroscopy (FT-IR). In many scientific disciplines, including chemistry, materials science, pharmaceuticals, and forensics, it has evolved into a crucial tool.

The analysis sample's ability to absorb infrared light forms the basis of FT-IR spectroscopy. Some of the infrared light that enters the material is absorbed by the molecules, but the rest is still able to pass through. By measuring the intensity of the transmitted light as a function of wavenumber, which stands for the energy of the infrared radiation, the resulting spectrum is obtained.

The spectrum produced by FT-IR analysis gives the material under investigation a distinct chemical fingerprint. It has several bands or peaks, each of which corresponds to a different vibrational mode of the molecules in the sample. These vibrational modes result from the bending and stretching of the molecules' chemical bonds.[19]

Depending on how the atoms move, the stretching vibrations can be further divided into symmetric and asymmetric types. While the atoms move in opposite directions during an asymmetric stretch, they do so simultaneously during a symmetric stretch. Bond angle changes occur during bending vibrations.[20]

The location, magnitude, and shape of these bands in the FT-IR spectrum reveal important

details about the sample's molecular make-up, functional groups, and chemical surroundings. The compounds present in the material can be identified by scientists by comparing the obtained spectrum with reference spectra or by using spectral databases.

FT-IR spectroscopy has a number of benefits. It requires little sample preparation and is non-destructive. Solids, liquids, and gasses can all be subjected to its analysis. Due to its high sensitivity, even minute amounts of compounds can be detected. It also offers data on the sample that is both quantitative and qualitative.

In conclusion, FT-IR spectroscopy is an effective and flexible method for characterizing, identifying, and analyzing chemicals. By giving each molecule a distinct spectral fingerprint, it enables researchers to decipher the complexities of molecular structure and composition in a variety of applications.



Fig. 2.3. Fourier infrared transform spectroscopy

2.4 Scanning electron microscope (SEM)

An effective method for examining the morphologies of various samples and substances is scanning electron microscopy (SEM). SEM uses an electron beam to deliver precise data to researchers about the surface traits, appearance, structure, and arrangement of materials.

The sample is subjected to a raster scanning approach during the SEM process, in which the electron beam moves back and forth across the sample's surface in a deliberate pattern. When the thermal energy exceeds the reference element's work function, the beam, produced by an electron source, is released. The anode then activates and excites the beam, giving it a positive charge.

The entire electron column, including the sample, is set up in a vacuum environment to ensure precise observations and reduce interference. In addition to shielding the electron column from debris, vibrations, and noise, this vacuum also makes high-resolution imaging possible and improves the detector's ability to gather electrons.[21]

Electromagnetic lenses, which typically consist of an objective lens and a condenser lens, direct the path of the electrons inside the SEM. The objective lens concentrates the electron beam onto the specimen for accurate imaging and analysis, while the condenser lens collects the electron beam and controls its intensity.

SEM creates precise images and data about the topography, morphology, structure, and crystallography of the material by scanning the sample surface and identifying the signals produced by the interaction between the electrons and atoms in the specimen. In numerous fields of science and industry, this information has many uses.



Fig. 2.4. Scanning electron microscope

SEM is a crucial tool in materials science for characterizing and analyzing the microstructure of materials, giving researchers insights into the configuration of particles, grain boundaries, and flaws. It is frequently used to look into the morphology and quality of semiconductor materials in research and development.[22] SEM is used in the study of nanomaterials, such as nanoparticles and nanofibers, in the field of nanotechnology, enabling accurate measurements and characterization at the nanoscale.

SEM is essential for examining the surface morphology of biological samples, such as cells, tissues, and organisms, in biology and the life sciences. It aids in the visualization of complex biological structures like cell membranes, organelles, and microorganism surface features.[23]

SEM also has uses in geology, archaeology, forensic science, and material failure analysis, among other fields. It is a flexible tool that supports comprehension of the characteristics and behavior of various materials across disciplines.

In conclusion, scanning electron microscopy is a useful method for examining the complex world of surface morphologies and structures. SEM provides detailed information that contributes to advancements in a variety of scientific, technological, and industrial fields by utilizing the power of electron beams and electromagnetic lenses.

2.5 Photoluminescence (PL) spectroscopy

A potent method for examining the characteristics of different materials for light emission is photoluminescence spectroscopy. It provides deeper insights into the dynamic behavior and excited state processes of luminescent systems when combined with time-dependent measurements. Time-dependent photoluminescence (PL) analysis offers a wealth of knowledge that goes beyond steady-state measurements in this situation.

The temporal evolution of the photoluminescence emission can be studied by using time-resolved methods like time-correlated single photon counting (TCSPC) or streak camera measurements. Thus, phenomena like exciton dynamics, carrier recombination, radiative and non-radiative decay, and energy transfer pathways can all be studied.

The determination of important parameters like the excited-state lifetime is possible with time-dependent photoluminescence measurements. The average amount of time a material spends in the excited state before transitioning back to the ground state and emitting a photon is represented by the excited-state lifetime. Understanding the effectiveness and behavior of luminescent materials requires knowledge of this information.

Additionally, time-resolved PL offers insightful knowledge into the underlying processes that affect the emission properties. The efficiency of the luminescence, for instance, may be affected by the presence of trap states, which are energy levels within the material that have the ability to capture and release charge carriers. The type and density of these trap states can be identified by examining the decay kinetics.

Additionally, the interaction between the luminescent material and its surroundings can be

clarified by time-dependent PL experiments. For instance, researchers can examine the behavior of thermal quenching, investigate energy transfer processes, and judge the stability of the material under various circumstances by varying the temperature or applying external stimuli.[24]

The dynamic behavior of luminescent materials can be thoroughly understood through time-dependent photoluminescence spectroscopy, in general. It offers priceless details on excited-state dynamics, emission kinetics, and the impact of outside variables. Researchers can obtain both spatial and temporal information by combining this method with spatially resolved micro-PL, allowing for detailed mapping of the photoluminescent properties throughout a sample. This multifaceted strategy aids in the creation and improvement of luminescent materials for a variety of applications, such as optoelectronics, sensing, and photonics.

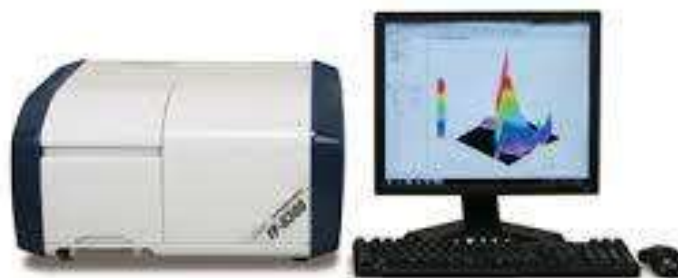


Fig.2.7. Photoluminescence spectroscopy

2.6 Decay time

A fascinating phenomenon known as photoluminescence decay happens when a substance absorbs photons and then releases light. In a number of disciplines, including physics, chemistry, and materials science, this process is frequently seen. Characterizing and examining luminescent materials and their applications requires an understanding of the photoluminescence decay behavior.

When an external light source, like a laser or strong radiation, excites a material, the absorbed energy promotes electrons to higher energy levels. Before quickly reverting to their ground state, these excited electrons stay in this energized state for a brief period of time. They undergo a transition back and emit photoluminescence, which is the release of extra energy as light.

An emission intensity as a function of time is shown by a decay curve, which can be used to describe the decay of photoluminescence. The intensity of this curve typically decreases quickly at first, then slowly until it reaches a steady-state or background level. The radiative and non-radiative decay pathways, as well as the material's overall luminescence efficiency, can all be inferred from the shape of the decay curve.

When the photoluminescence decay curve displays multi-exponential behavior, it means that there are several decay pathways with various characteristic lifetimes. Multiple factors, including flaws, impurities, or various emission centers within the material, contribute to this complexity. Researchers can learn more about the material's composition, structure, and optical properties by examining the decay curve and extracting the lifetimes connected with various decay components.[25]

Using methods like time-resolved spectroscopy, which uses ultrafast lasers and detectors to capture the transient emission signals with high temporal resolution, photoluminescence decay and its corresponding curve are extensively studied. By helping to develop new luminescent materials, optoelectronic devices, and cutting-edge imaging methods, these experiments enable researchers to better understand the mechanisms governing the photoluminescence process.

To sum up, a wealth of knowledge about the luminescent behavior of materials can be gleaned from the photoluminescence decay and its curve. Understanding the fundamental characteristics of light-emitting systems and designing and optimizing various technologies in industries ranging from energy conversion to biomedical imaging both benefit greatly from the analysis of these decay curves.

CHAPTER 3:

EXPERIMENTAL PROCEDURE

3.1 Synthesis: Sol Gel method

A flexible and popular method for creating phosphors with specific properties for a variety of applications is the sol-gel method. The sol-gel method, in contrast to the solid-state reaction method, begins with a sol, a colloidal suspension of inorganic precursors in a liquid medium, usually an alcohol or water.

The inorganic precursors that are desired are dissolved in the liquid medium under carefully controlled conditions to create a sol, which is the first step in the synthesis process. Precursors are chosen according to the desired properties and the specific phosphor being synthesized. To ensure the formation of a homogeneous and stable colloidal suspension, the sol is carefully prepared.[26]

Once the sol is ready, it goes through a process called gelation that causes a three-dimensional network of connected nanoparticles to form. Different techniques, such as chemical reactions, pH adjustments, or temperature changes, can cause gelation. The final morphology and structure of the phosphor are determined by the gelation process, which is essential.

After gelation, the produced gel is aged and dried to get rid of the solvent and make a solid. To avoid cracking or unintended phase transitions, drying is frequently done at a controlled temperature. After drying, the produced gel is heated at a high temperature during a process called calcination. The process of calcination makes it easier to remove any remaining organic materials and encourages the formation of the desired phosphor phase.

For the synthesis of phosphors, the sol-gel method has a number of benefits. It enables fine-grained control over the morphology, composition, and size of the phosphor. Incorporating dopants and creating composite materials are also made possible by the sol-gel method, broadening the range of phosphor properties that can be achieved. In addition to being low temperature, energy-efficient, and environmentally friendly, the process.[27]

In conclusion, the sol-gel method is a very flexible and effective technique for phosphor synthesis. It is possible to create phosphors with tailored properties suitable for a variety of applications, such as lighting, displays, and optoelectronic devices, by meticulously controlling the sol-gel process parameters.

3.2 Sample preparation: SrMgSi₂O₆

The preparation of Sm³⁺ doped Strontium Magneto Silicate (SMSS) SrMgSi₂O₆ was

carried out using sol-gel method. For the synthesis, the masses of high purity reactants such as magnesium nitrate hexahydrate ($\text{Mg}(\text{NO}_3)_2 \cdot 6\text{H}_2\text{O}$), silicon dioxide (SiO_2), strontium nitrate ($\text{Sr}(\text{NO}_3)_2$), samarium oxide (Sm_2O_3) and citric acid ($\text{C}_6\text{H}_8\text{O}_7$) are calculated and dissolved in de-ionized water.[28] For the SMSS sample synthesis, all of the reactants are then mixed together. The mixture is stirred in a magnetic stirrer for 1 hr. at 80 °C and then at 110 °C until gel is formed. To produce a powder composition, the gel is then dried and crushed into powder form in a motor pestle. The powder is then sintered in an alumina crucible in a furnace at a temperature of 400 °C for 2 hr. and then at increased temperature of 1000 °C for 6hr. The resultant white colored powder is then crushed and was used for characterisation.

3.3 Analysis of sample

The SMSS phosphor were made using varying mol percent values of Sm^{3+} doping. An X-ray diffractometer was utilized to examine the crystalline properties of these materials (Bruker: model D8 advance). It uses nickel filtered $\text{CuK}\alpha$ ($\lambda = 1.541 \text{ \AA}$) to scan the sample at an angle of 2θ ranging from 10° to 80° . With the help of a JASCO spectrophotometer, bandgap studies are carried out (Model no. V-770). The Perkin Elmer Spectrum Two FT-IR spectrometer was utilized to explore the bonding modes in the crystal lattice in the region of 400 to 1600 cm^{-1} . The morphological findings were investigated utilizing a Zeiss GeminiSEM 500 scanning electron microscope. The photoluminescence properties were measured using a Shimadzu RF-5301 PC Spectrofluorophotometer. The excitation and emission spectra were captured using a JASCO FP-8300 fluorescence spectrophotometer and an excitation source (Xenon lamp).

CHAPTER 4:

RESULTS AND DISCUSSION

4.1 Structural studies

X-ray Diffraction studies for SMSS samples that were un-doped (0.0), doped at 1.0, 2.0, 3.0, 4.0, and 5.0 mol% Sm^{3+} were compared to baseline data. Sharp and single peaks were clearly visible in the XRD patterns. This demonstrates that the sample has crystallized effectively and suggests that a single-phase polycrystalline nature has formed. The pure phase formation of Sm^{3+} doped SMSS phosphors is confirmed by the indexing of all existing diffraction peaks in XRD patterns to standard JCPDS data (01-075-1736).

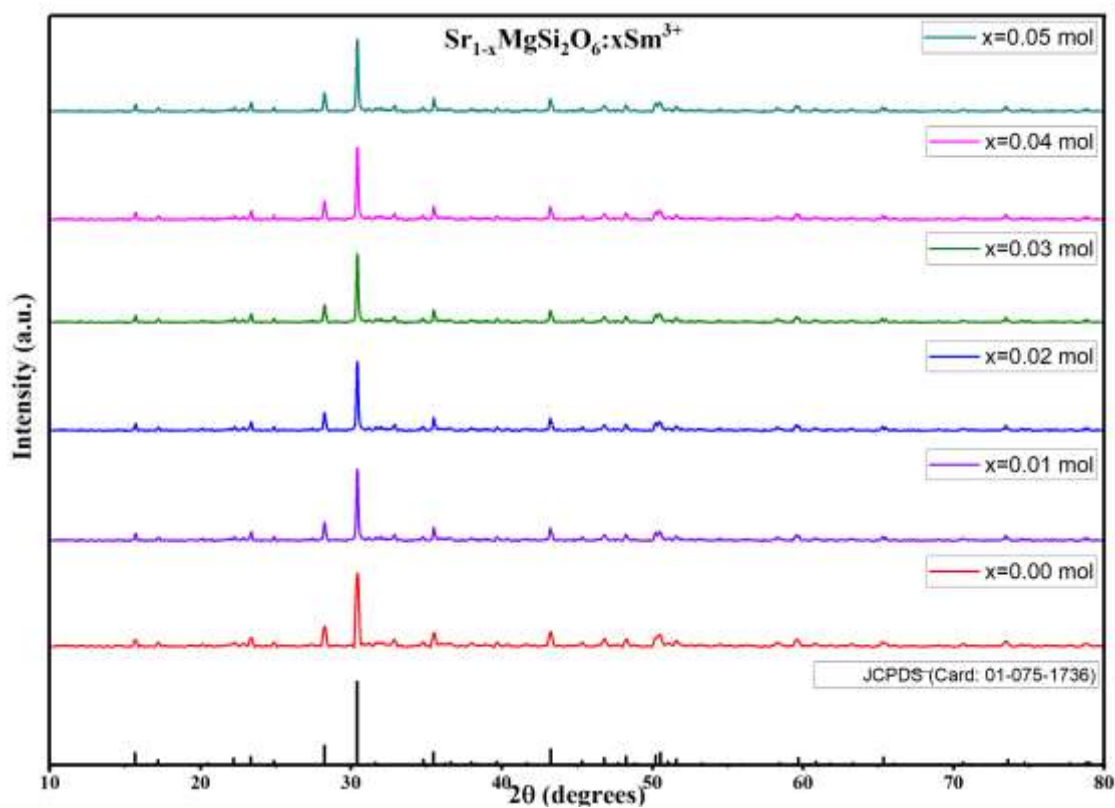


Fig. 4.1. XRD patterns of SMSS phosphor at different concentration of Sm^{3+} doped SMSS phosphor

4.2 Diffuse Reflectance Spectroscopy

The UV-Vis diffuse reflectance spectrum of Sm^{3+} doped $\text{SrMgSi}_2\text{O}_6$ phosphor series was analyzed in the 240-1400 nm range, revealing the presence of near-ultraviolet (n-UV) and blue regions, which was attributed to the f-f transitions of Sm^{3+} ions. The DR spectra revealed a distinct absorption edge at 260 nm across all concentration levels, indicating the presence of an energy band gap.[29]

In the longer wavelength region, several weak absorption peaks were observed at specific wavelengths: 948 nm, 1080 nm, 1232 nm, and 1380 nm. These peaks corresponded to electronic transitions from the common ground state ${}^6H_{5/2}$ to the excited states ${}^6F_{5/2}$, ${}^6F_{7/2}$, ${}^6F_{9/2}$, and ${}^6F_{11/2}$ of the Sm^{3+} ions embedded within the phosphor lattice. These transitions signify the ability of the Sm^{3+} ions to absorb light energy and transition to higher energy states.[30]

Conversely, at shorter wavelengths, an absorption band ranging from 340 nm to 480 nm was observed. This absorption band was attributed to the 4f-4f transitions of the Sm^{3+} ions, indicating the involvement of the 4f electron orbitals in the absorption process.

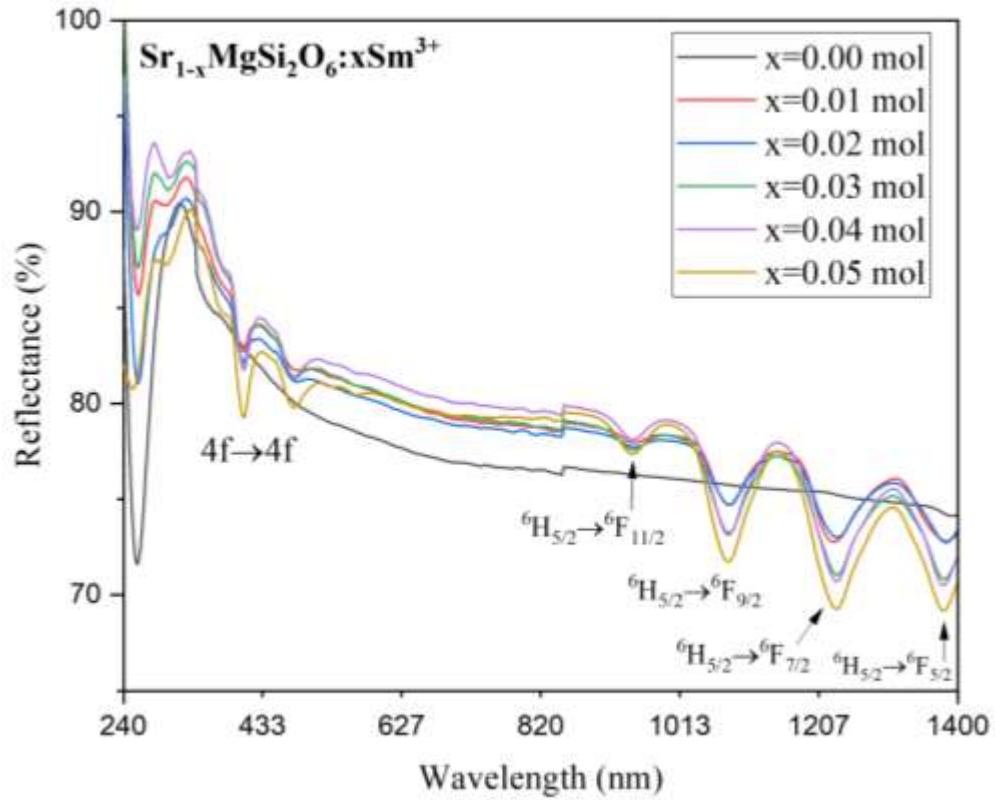


Fig. 4.2. UV diffuse reflectance spectra of undoped and Sm^{3+} doped SMSS phosphor

In order to assess the energy band gap of the phosphor material at the optimal molar concentration of Sm^{3+} (2 mol. %), the spectrum was transformed into the Kubelka-Munk function $F(R)$, or absolute reflectance, using the equation:[31]

$$F(R) = \frac{(1-R)^2}{2R} \quad (2)$$

Next, the absolute reflectance ($F(R)$) was employed as a substitute for the absorption coefficient (α) in the equation

$$(\alpha h\nu)^2 = B(h\nu - E_g) \quad (3)$$

where h represents Planck's constant, ν denotes frequency, E_g stands for the energy band gap, B represents the band tailing parameter, and n indicates the nature of the transition (direct/indirect, allowed/forbidden).

To determine the energy band gap, a Tauc plot was constructed by plotting $(F(R)h\nu)^n$ against $h\nu$. The value of n was considered 2 for indirect transitions.[32] By extrapolating the linear region of the plot to intersect the x-axis, the estimated values for indirect energy band gap was found to be 4.39 eV.

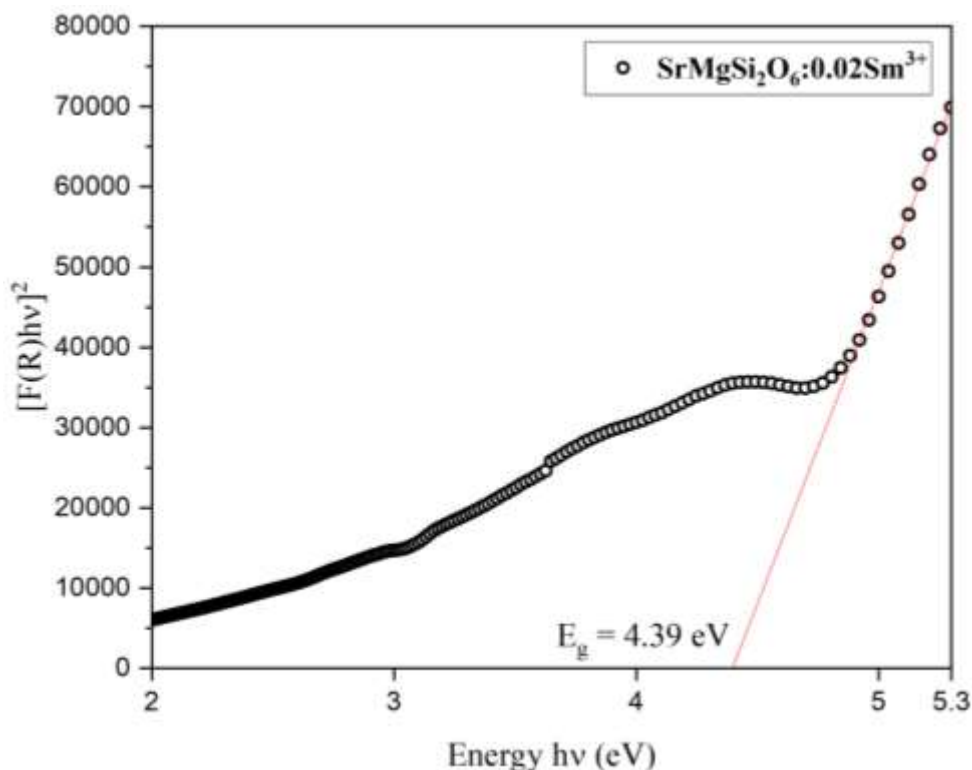


Fig. 4.3. Energy band gap of 2.0 mol% Sm³⁺ doped SMSS phosphor

4.3 Fourier transform infrared spectroscopy

The FT-IR spectrum analysis of the prepared phosphor material reveals several characteristic bands that provide valuable insights into its molecular composition and structure and reveals distinct absorption bands that indicate the presence of silicate groups. Upon careful examination, we can identify various functional groups and ions present in the sample.

One prominent feature in the spectrum is an intense band centered at 838 cm^{-1} , along with another band at 919 cm^{-1} . These bands are assigned to the asymmetric stretching vibration of the Si-O-Si bonds in the silicate groups. The presence of these bands strongly suggests the existence of silicate compounds within the sample. associated with the asymmetric stretching of the Si-O-Si bonds[33]

The symmetric stretching vibration of the Si-O bonds (Si-O) in the silicate groups is also visible as a band at 669 cm^{-1} . This provides more evidence that silicate compounds are present in the substance.

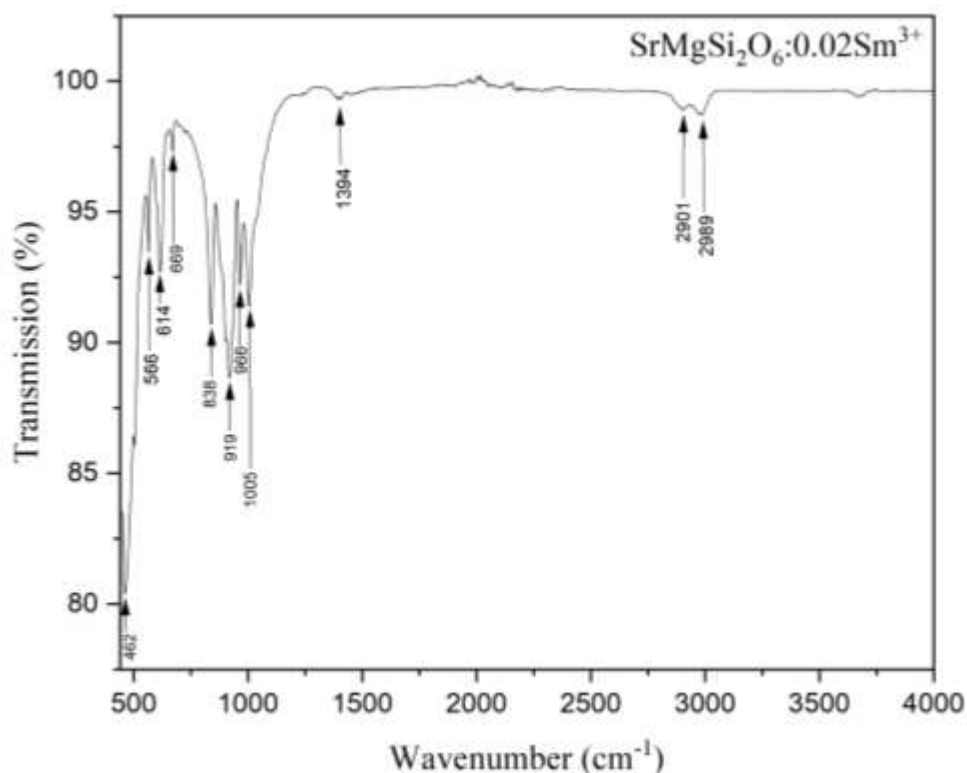


Fig. 4.3. FT-IR patterns of 2.0 mol% Sm^{3+} doped SMSS phosphor

It's interesting to note that the bending vibrations of Mg-O bonds can also be responsible for the band at 838 cm^{-1} . This suggests that magnesium-oxygen bonds are present within the silicate structure and may even be present as a silicate compound itself.

The spectrum also shows bands at 566 cm^{-1} and 462 cm^{-1} , which are attributed to the Si-O-Si bonds' vibrational mode of bending. These bands offer additional proof that the material contains silicate groups.

The bands centered at 566 cm^{-1} , 614 cm^{-1} , 669 cm^{-1} , 838 cm^{-1} , 966 cm^{-1} and 1005 cm^{-1} can all be attributed to the SiO_4 group, which is a characteristic unit of silicate compounds. The presence of these bands further confirms the existence of silicate compounds in the sample.[34]

The analysis of the FT-IR spectrum offers convincing proof that the material contains silicate groups. We can better understand the molecular makeup and composition of the sample under study by taking into account the assigned bands for the stretching and bending vibrations of the Si-O-Si and Si-O bonds as well as the presence of the SiO_4 group.

4.4 Morphological studies

Scanning electron microscopy (SEM) was used to analyze the surface morphology and particle sizes. The phosphor samples can be seen in more detail in the resulting SEM images.

The $\text{SrMgSi}_2\text{O}_6:0.02\text{Sm}^{3+}$ phosphors exhibit a distinctive surface morphology, as shown by the SEM micrographs. The image is dominated by solid microcrystalline structures, which point to the synthesized material's well-formed and compact nature. But between the crystalline grains, there is some agglomeration that was probably brought on by the high-temperature reaction process. The overall micrographs show a stable and cohesive phosphor structure despite the agglomeration.[35]

Additionally, the SEM images shed light on the phosphors' particle sizes. The enlarged micrograph indicates that the size of the particles generally falls within the micrometer range. The SEM images can be further examined to produce more accurate measurements of the particle dimensions. Understanding the physical characteristics and potential uses of the synthesized $\text{SrMgSi}_2\text{O}_6:0.02\text{Sm}^{3+}$ phosphors depends on this information.

Applications in illumination, displays, and lighting are ideal for this phosphor. The phosphors' ease of substrate adhesion makes it possible for them to be seamlessly integrated into a variety of systems and devices, improving their performance and functionality

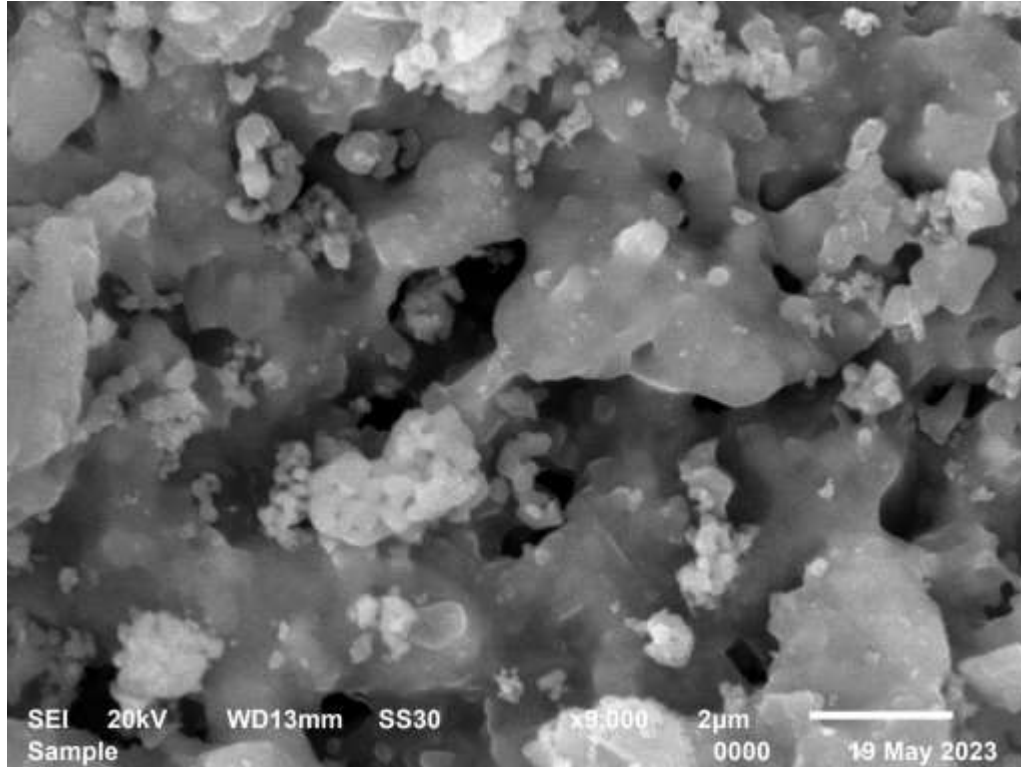


Fig. 4.5. SEM micrographs of SMSS Phosphor

4.5 Photoluminescence spectra

4.5.1 Excitation spectra

The emission at a specific wavelength of 601 nm was observed in order to analyze the excitation spectra of Sm^{3+} doped $\text{SrMgSi}_2\text{O}_6$ phosphors. The excitation spectra that were obtained showed a number of distinct peaks centered at various wavelengths. These peaks show that blue and near-ultraviolet (n-UV) light sources effectively excite the Sm^{3+} ions. As a result of the presence of multiple excitation peaks, it is possible to access a variety of energy levels and create flexible excitation mechanisms.

Among the observed excitation peaks, the peak corresponding to the ${}^6\text{H}_{5/2} \rightarrow {}^4\text{F}_{7/2}$ transition exhibited the highest excitation intensity. This suggests that efficient emission can be achieved when the Sm^{3+} ions are excited at a wavelength of 404 nm, corresponding to this particular excitation peak. The intensity of this excitation peak indicates the likelihood of successful excitation and subsequent emission in the phosphor material.[36][37]

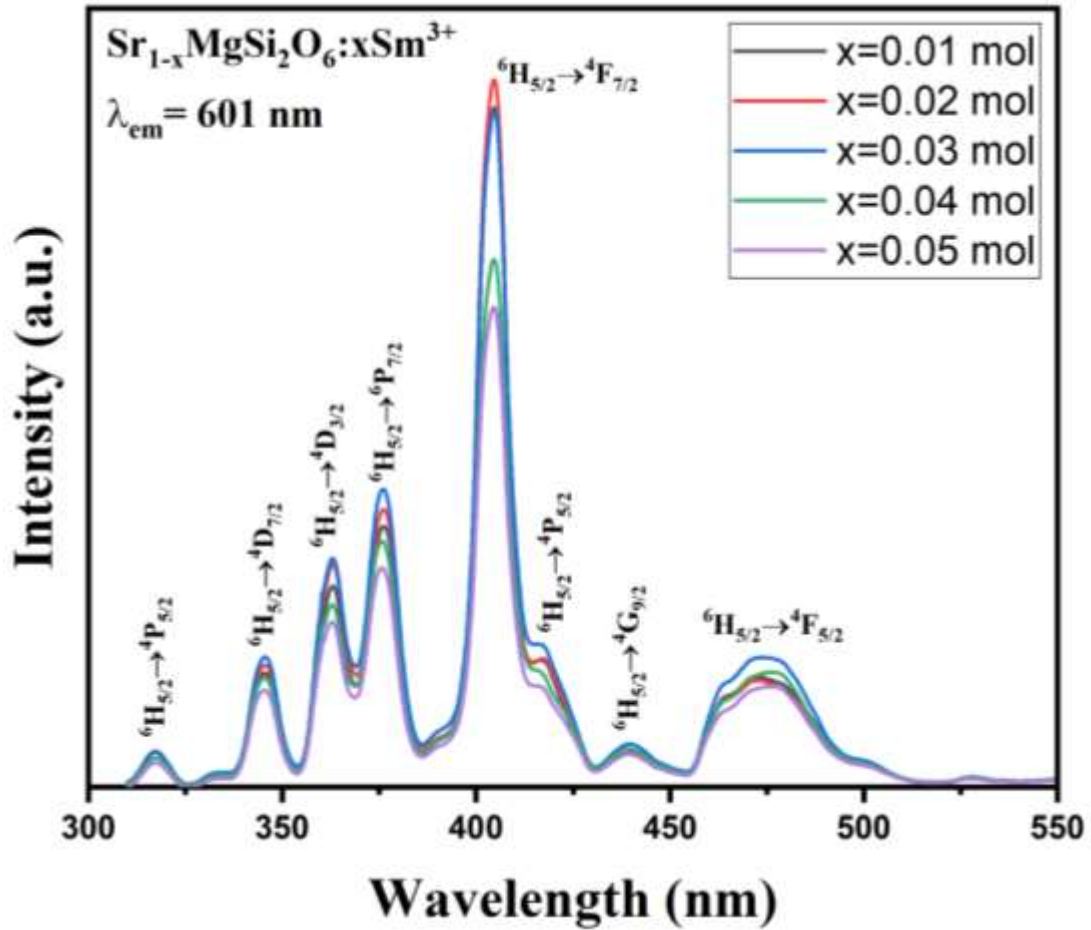


Fig. 4.6. PLE spectrum of Sm^{3+} doped SMSS phosphor at 601 nm emission wavelength

4.5.2 Emission spectra

Moving on to the emission spectra, they were obtained by exciting the phosphors at the wavelength of 404 nm, which corresponds to the excitation peak with the highest intensity. The emission spectra exhibited distinct bands centered at wavelengths of 564 nm, 601 nm, 646 nm and 708 nm. Among these, the emission at 601 nm, resulting from the ${}^4\text{G}_{5/2} \rightarrow {}^6\text{H}_{7/2}$ transition, displayed the highest intensity.

The luminescence characteristics of Sm^{3+} ions in the $\text{SrMgSi}_2\text{O}_6$ host lattice are strongly influenced by the coordination symmetry of the surrounding environment. This coordination symmetry can lead to the splitting of energy levels and subsequent splitting of emission peaks, known as the Stark effect. In the emission spectra, the observed splitting of the peaks corresponds to the different Stark sublevels associated with the ${}^{2S+1}\text{L}_J$ multiplet, where S represents the total spin and J represents the total angular momentum. For an odd number of electrons in an f orbital, the highest possibility of Stark sublevels for a given multiplet is

$(2J+1)/2$. Consequently, Stark splitting is observable for J values of 5/2, 7/2, 9/2 and 11/2 as depicted in the emission spectra.[37]

The emission transitions in the phosphors can be classified as magnetic dipole and electric dipole transitions based on the selection rule established by Laporte. The ${}^4G_{5/2} \rightarrow {}^6H_{7/2}$ transition, characterized by a ΔJ value of 0, is a magnetic dipole transition. On the other hand, the transitions involving the ${}^4G_{5/2} \rightarrow {}^6H_{5/2}$ and ${}^4G_{5/2} \rightarrow {}^6H_{9/2}$ transitions are electric dipole transitions, following the selection rule $\Delta J' \leq 6$, where J or J'=0 and $\Delta J=2, 3, 6$. The emission intensity ratio between electric dipole and magnetic dipole transitions provides valuable information about the site symmetry surrounding the Sm^{3+} ions. In this particular study, the emission intensity of the magnetic dipole transition was found to be higher than that of the electric dipole transition, indicating a symmetric environment surrounding the Sm^{3+} ions within the $SrMgSi_2O_6$ lattice. The relatively lower intensity ratio for the electric and magnetic dipole transitions also suggests a lesser degree of distortion from the inversion symmetry.[38]

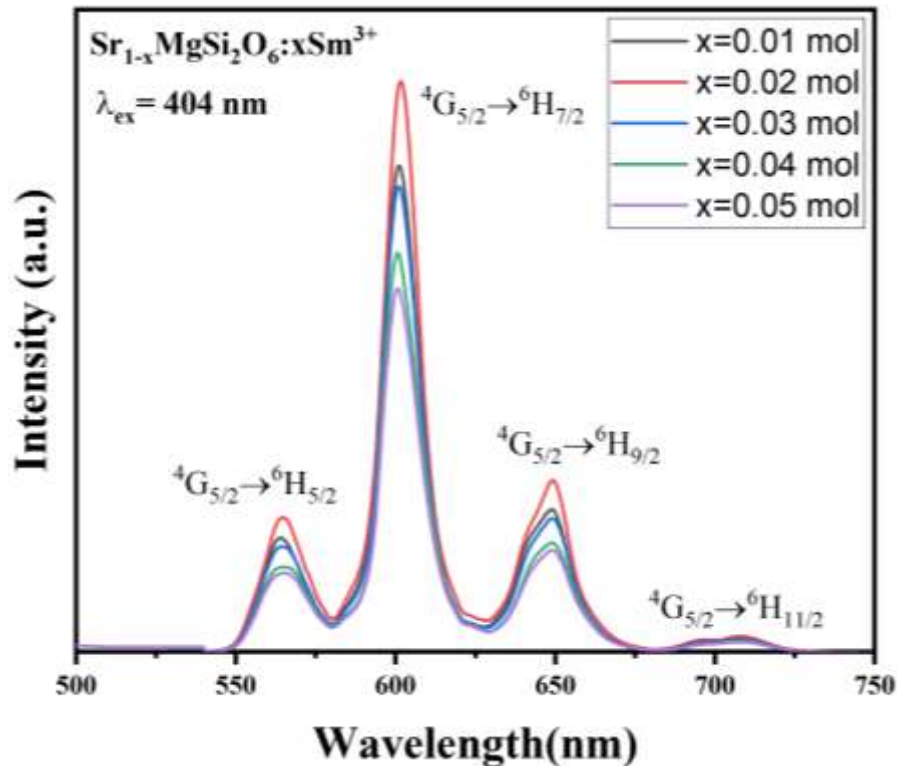


Fig. 4.7. Emission spectra of Sm^{3+} doped SMSS phosphor at 404 nm excitation wavelength

In addition to studying the excitation and emission characteristics, the effect of Sm^{3+} ion concentration on the luminescence behavior of the $SrMgSi_2O_6$ phosphors was investigated.

The concentration of Sm^{3+} ions was varied in the host lattice, and its impact on the emission intensity was examined. It was observed that the emission intensity initially increased as the Sm^{3+} concentration was increased from 0.01 to 0.02 mol.

However, beyond this critical concentration of 0.02 mol, known as concentration quenching, the emission intensity started to decrease. At higher concentrations, non-radiative energy transfer processes between Sm^{3+} ions are responsible for this behavior. The likelihood of non-radiative energy transfer becomes predominant when the Sm^{3+} ions are too close to one another, which lowers the overall luminescence efficiency. As a result, 0.02 mol of Sm^{3+} was found to be the ideal concentration for the $\text{SrMgSi}_2\text{O}_6$ phosphor to produce the highest emission intensity.

4.6 Temperature Dependent Photoluminescence

An extensive investigation was carried out with a focus on temperature-dependent photoluminescence (PL) studies to evaluate the $\text{SrMgSi}_2\text{O}_6$ phosphor's thermal stability. After being optimized, the phosphor was excited at 404 nm. Analysis of the data obtained showed that the PL intensity gradually decreased as the temperature rose above room temperature (RT).

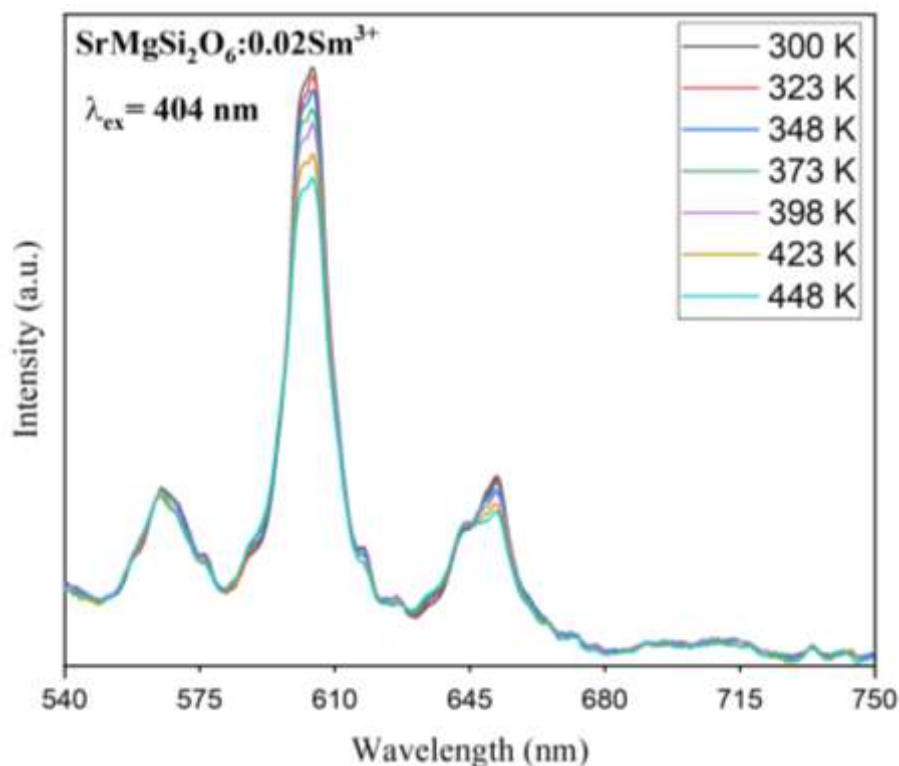


Fig. 4.8. Temperature dependent photoluminescence of 2.0 mol% Sm^{3+} doped SMSS phosphor at 404 nm excitation wavelength

Further examination allowed for a more detailed observation of the PL intensity at specific temperatures. Notably, at 423 K and 448 K, the phosphor maintained 85.9% and 82.1% of the PL intensity observed at RT, respectively. This decline in PL intensity can be attributed to the heightened thermal energy, causing electrons to undergo non-radiative transitions between the excited and ground states, resulting in energy dissipation rather than radiative emission.[39]

To dive deeper into the phosphor's thermal stability, the activation energy using the Arrhenius equation is calculated using the following equation:

$$I_T = \frac{I_0}{1 + C \exp\left(\frac{-\Delta E}{K_B T}\right)} \quad (4)$$

Here, I_0 and I_T represent the PL intensity at RT and temperature T (in Kelvin), respectively. The activation energy is denoted by E, while K_B signifies Boltzmann's constant (8.67×10^{-5} eV/K), and C represents an arbitrary constant.[40]

$$\ln\left[\left(\frac{I_0}{I_T}\right) - 1\right] = -\frac{\Delta E}{K_B T} + C \quad (5)$$

By plotting $\ln[(I_0/I_T)-1]$ against $(1/K_B T)$ and analyzing the slope of the resulting linear fit, the activation energy is found to be 0.268 eV. This higher activation energy value signifies an enhanced thermal stability for the synthesized phosphor

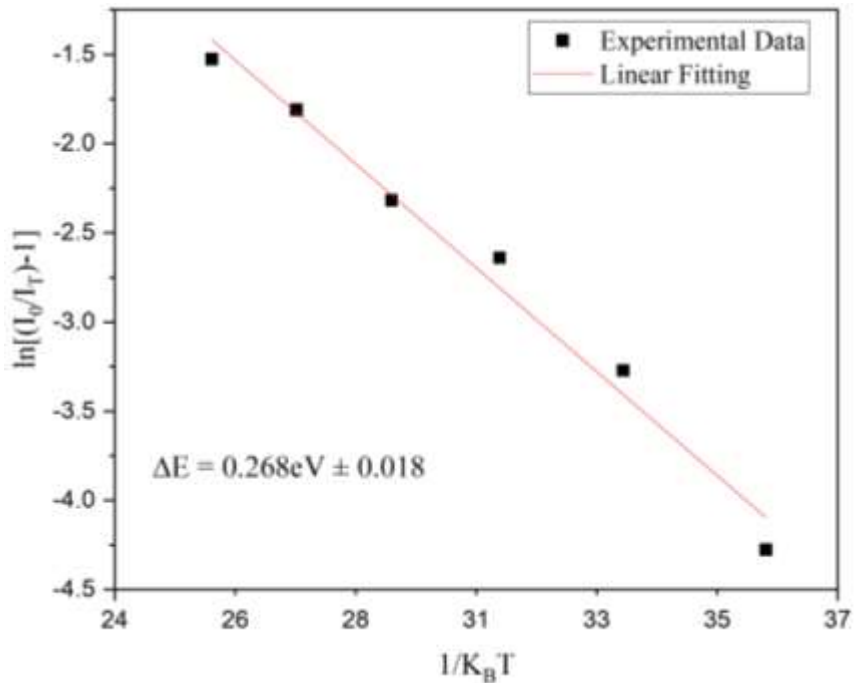


Fig. 4.9. Plot for Activation Energy

4.7 Color chromaticity diagram for SMSS

The CIE coordinates (0.592, 0.406) are clearly located in the pure orange region of the CIE 1931 diagram for a 2.0 mol% Sm^{3+} ion doped SMSS phosphor when evaluated under 404 nm excitation. This shows that the phosphor emits light primarily in the orange range when excited at 404 nm.

CIE 1931

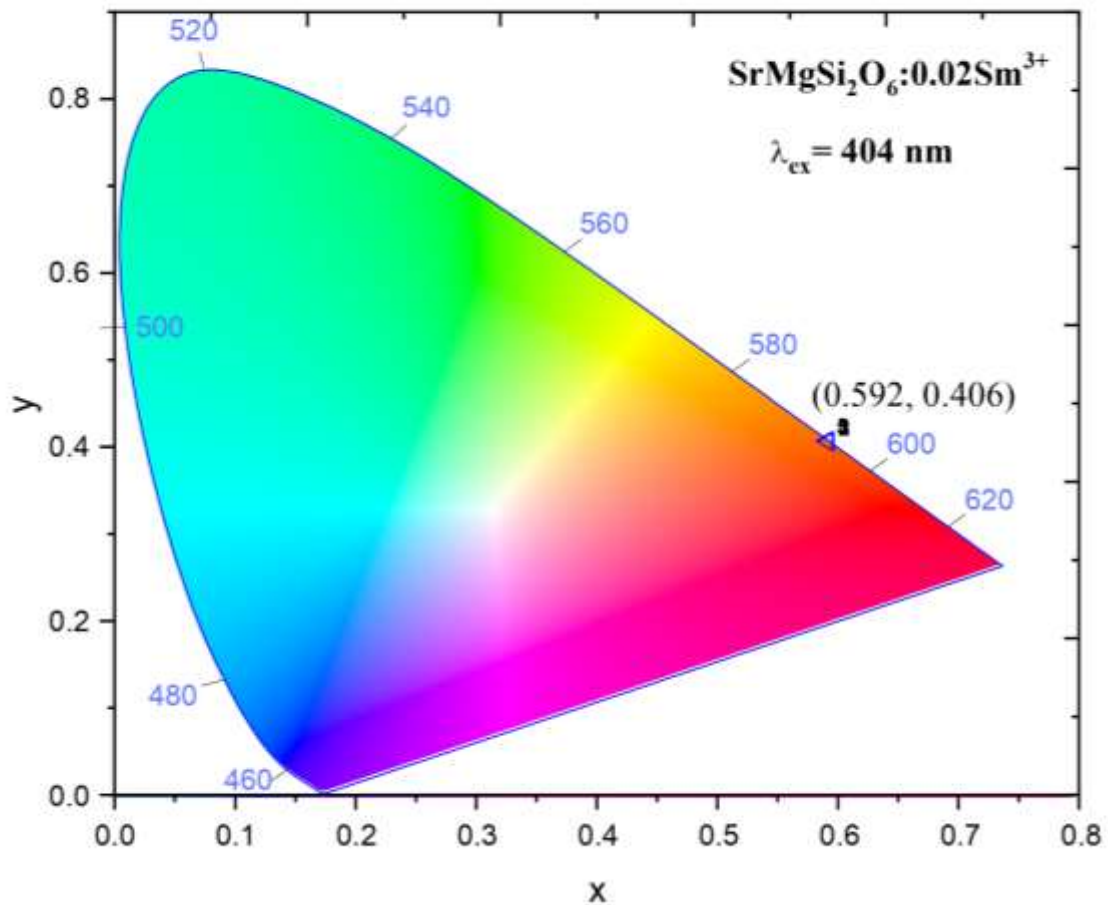


Fig. 4.10. CIE chromaticity diagram of 2.0 mol% of Sm^{3+} doped SMSS phosphor under excitation wavelengths of $\lambda_{\text{ex}}=404 \text{ nm}$

CHAPTER 5:

CONCLUSIONS

CONCLUSIONS

The Sol-gel method was used to synthesize high-quality $\text{SrMgSi}_2\text{O}_6:\text{Sm}^{3+}$ phosphor, and its structural and photoluminescence characteristics have been thoroughly characterized. The phosphor is single phase and exhibits excellent crystallization, according to the analysis of powder X-ray diffraction (XRD). This shows that the desired material was successfully formed. Scanning electron microscopy (SEM) analysis of the morphology of the phosphor revealed an irregular structure. The surface of the phosphor was found to contain submicron-sized agglomerates of SMSS, as seen in the SEM micrographs. The performance and characteristics of the phosphor are significantly impacted by this morphology. The excitation and emission spectra of the phosphor have been used to analyze its luminescent behavior. The phosphor was excited at 404 nm, and distinct emission peaks were seen that corresponded to particular transitions of the samarium ions. The optimal concentration of Sm^{3+} ions, 2.0 mol%, produced the strongest reddish-orange emission. Higher dopant concentrations, however, led to the presence of concentration quenching effects. The SMSS phosphor was excited by blue and near-ultraviolet (n-UV) light and released an orange light at a wavelength of 601 nm. The emission spectra showed that the phosphor's color coordinates were located in the orange region. This demonstrates the phosphor's potential for use in phosphor-converted white light-emitting diodes (pc-wLEDs), which are inexpensive LEDs. The $\text{SrMgSi}_2\text{O}_6:\text{Sm}^{3+}$ phosphor's suitability for pc-wLED applications was further supported by the CIE chromaticity coordinates derived from the emission spectra. The coordinates' representation of its orange emission is in line with the qualities that will produce high quality white light.

CHAPTER 6:

SCOPE OF WORK

SCOPE OF WORK

Samarium (Sm^{3+}) have been successfully doped into SMSS host material, which has been the focus of recent work. As a result, high purity phosphor that can be used to create inexpensive phosphor-converted white light-emitting diodes (pc-wLEDs) was synthesized. Various opto-electronic devices are also among the potential uses of these phosphors.

Co-doping strategies with additional compatible rare-earth ions (RE) can be investigated to further improve the luminescent properties of these phosphors. Elements like yttrium (Y^{3+}), gadolinium (Gd^{3+}), terbium (Tb^{3+}), and lutetium (Lu^{3+}) have shown promising results.

These SMSS phosphors were primarily synthesized using the Sol-gel method, along with thorough structural and photoluminescence characterization. Alternative synthesis techniques, like the traditional solid-state reaction method, offer a chance to enhance particle morphology and shrink particle size. A distinctive black fluffy structure that can be further sintered at different temperatures is produced by the combustion method, which uses metal nitrates as precursors and subjects them to high-temperature combustion. Investigating the combustion process may reveal greater potential for improving the luminescent qualities of the synthesized phosphors.

Beyond their use in wLEDs, these phosphors have a wide range of applications. Their adaptability opens up opportunities for opto-electronic applications such as thermal sensing, bioimaging, and fingerprint sensing, among others. We can create prototype wLEDs designed especially for these various applications by optimizing these phosphors.

REFERENCES

- [1] Le, T. C., & Winkler, D. A. (2016). Discovery and Optimization of Materials Using Evolutionary Approaches. *Chemical Reviews*, 116(10), 6107–6132. <https://doi.org/10.1021/acs.chemrev.5b00691>
- [2] Toledo-Martín, E. M., García-García, M. del C., Font, R., Moreno-Rojas, J. M., Salinas-Navarro, M., Gómez, P., & del Río-Celestino, M. (2018). Quantification of Total Phenolic and Carotenoid Content in Blackberries (*Rubus Fruticosus* L.) Using Near Infrared Spectroscopy (NIRS) and Multivariate Analysis. *Molecules*, 23(12). <https://doi.org/10.3390/molecules23123191>
- [3] Chung, H., Zhou, C., Tee, X. T., Jung, K.-Y., & Bermel, P. (2016). Hybrid dielectric light trapping designs for thin-film CdZnTe/Si tandem cells. *Opt. Express*, 24(14), A1008–A1020. <https://doi.org/10.1364/OE.24.0A1008>
- [4] Kaur, S., Rao, A. S., Jayasimhadri, M., Sivaiah, B., & Haranath, D. (2019). Synthesis optimization, photoluminescence and thermoluminescence studies of Eu³⁺-doped calcium aluminozincate phosphor. *Journal of Alloys and Compounds*, 802, 129–138. <https://doi.org/https://doi.org/10.1016/j.jallcom.2019.06.169>
- [5] Zhao, M., Liu, Y., Ma, S., Liu, D., & Wang, K. (2018). Investigation of energy transfer mechanism and luminescence properties in Eu³⁺ and Sm³⁺ co-doped ZnWO₄ phosphors. *Journal of Luminescence*, 202, 57–64. <https://doi.org/https://doi.org/10.1016/j.jlumin.2018.05.030>
- [6] Fan, B., Liu, J., Zhou, W., & Han, L. (2019). Enhanced luminescence properties of Eu³⁺-doped high silica glass by Ag nanoparticles. *Journal of Luminescence*, 215, 116687. <https://doi.org/https://doi.org/10.1016/j.jlumin.2019.116687>

- [7] Jayachandiran, M., & Kennedy, S. M. M. (2019). Synthesis and optical properties of Ba₃Bi₂(PO₄)₄:Dy³⁺ phosphors for white light emitting diodes. *Journal of Alloys and Compounds*, 775, 353–359. <https://doi.org/10.1016/j.jallcom.2018.10.148>
- [8] Lin, C.-H., Huang, C.-H., Pai, Y.-M., Lee, C.-F., Lin, C.-C., Sun, C.-W., Chen, C.-H., Sher, C.-W., & Kuo, H.-C. (2018). Novel Method for Estimating Phosphor Conversion Efficiency of Light-Emitting Diodes. *Crystals*, 8(12). <https://doi.org/10.3390/cryst8120442>
- [9] Das, S., Amarnath Reddy, A., Surendra Babu, S., & Vijaya Prakash, G. (2011). Controllable white light emission from Dy³⁺–Eu³⁺ co-doped KCaBO₃ phosphor. *Journal of Materials Science*, 46(24), 7770–7775. <https://doi.org/10.1007/s10853-011-5756-5>
- [10] Ye, S., Xiao, F., Pan, Y. X., Ma, Y. Y., & Zhang, Q. Y. (2010). Phosphors in phosphor-converted white light-emitting diodes: Recent advances in materials, techniques and properties. *Materials Science and Engineering: R: Reports*, 71(1), 1–34. <https://doi.org/10.1016/j.mser.2010.07.001>
- [11] Lin, C. C., & Liu, R.-S. (2011). Advances in Phosphors for Light-emitting Diodes. *The Journal of Physical Chemistry Letters*, 2(11), 1268–1277. <https://doi.org/10.1021/jz2002452>
- [12] Ushakova, E. v, Cherevko, S. A., Kuznetsova, V. A., & Baranov, A. v. (2019). Lead-Free Perovskites for Lighting and Lasing Applications: A Minireview. *Materials*, 12(23). <https://doi.org/10.3390/ma12233845>
- [13] Nalwa, H. S., & Rohwer, L. (2003). *Handbook of Luminescence, Display Materials and Devices, 3-Volume Set* (Vol. 1).
- [14] Han, B., Dai, Y., Zhang, J., Liu, B., & Shi, H. (2018). Development of near-

- ultraviolet-excitable single-phase white-light-emitting phosphor
KBaY(BO₃)₂:Ce³⁺,Dy³⁺ for phosphor-converted white light-emitting-diodes. *Ceramics International*, 44(12), 14803–14810.
<https://doi.org/https://doi.org/10.1016/j.ceramint.2018.05.111>
- [15] Chateigner, D. (2006). Thin film analysis by X-ray scattering. By Mario Birkholz, with contributions by P. F. Fewster and C. Genzel. Pp. xxii+356. Weinheim: Wiley-VCH Verlag GmbH Co., 2005. Price (hardcover) EUR 119, SFR 188. ISBN-10: 3-527-31052-5; ISBN-13: 978-3-527-31052-4. *Journal of Applied Crystallography*, 39(6), 925–926.
<https://doi.org/10.1107/S0021889806034698>
- [16] le Bail, A. (2005). Whole powder pattern decomposition methods and applications: A retrospection. *Powder Diffraction*, 20(4), 316–326. <https://doi.org/DOI:10.1154/1.2135315>
- [17] Escobedo Morales, A., Sánchez Mora, E., & Pal, U. (2007). Use of Diffuse Reflectance Spectroscopy for Optical Characterization of Un-Supported Nanostructures. *67.Bf*, 53.
- [18] Banica, F.-G. (2012). Chemical Sensors and Biosensors: Fundamentals and Applications. In *Chemical Sensors and Biosensors: Fundamentals and Applications*.
<https://doi.org/10.1002/9781118354162>
- [19] Wong, K. C. (2015). Review of Spectrometric Identification of Organic Compounds, 8th Edition. *Journal of Chemical Education*, 92(10), 1602–1603.
<https://doi.org/10.1021/acs.jchemed.5b00571>
- [20] Ahamad, J., Ali, F., Sayed, M., Ahmad, J., & Nollet, L. (2022). *Basic Principles and Fundamental Aspects of Mass Spectrometry* (pp. 3–17).

<https://doi.org/10.1201/9781003091226-2>

[21] Kohl, H., & Reimer, L. (2008). Transmission Electron Microscopy. In *Transmission Electron Microscopy: Physics of Image Formation, Springer Series in Optical Sciences, Volume 36. Springer-Verlag New York, 2008* (Vol. 36).

<https://doi.org/10.1007/978-0-387-40093-8>

[22] Burany, S. (2003). Scanning Electron Microscopy and X-Ray Microanalysis. J. Goldstein, D. Newbury, D. Joy, C. Lyman, P. Echlin, E. Lifshin, L. Sawyer, and J. Michael. Kluwer Academic, Plenum Publishers, New York; 2003, 688 pages (Hardback, 75.00) ISBN 0-306-47292-9. *Microscopy and Microanalysis - MICROSC MICROANAL*, 9, 484. <https://doi.org/10.1017/S1431927603030617>

[23] Williams, D., & Carter, C. (2009). Transmission Electron Microscopy: A Textbook for Materials Science. In *Transmission electron microscopy. A textbook for materials science: Vol. III*. <https://doi.org/10.1007/978-1-4757-2519-3>

[24] Wu, Q., Dai, P., Wang, Y., Zhang, J., Li, M., Zhang, K. Y., Liu, S., Huang, W., & Zhao, Q. (2021). Time-resolved analysis of photoluminescence at a single wavelength for ratiometric and multiplex biosensing and bioimaging. *Chem. Sci.*, 12(33), 11020–11027. <https://doi.org/10.1039/D1SC02811A>

[25] Ariese, F., Roy, K., Venkatraman, R. K., Sudeeksha, H., Kayal, S., & Umapathy, S. (2017). *Time-Resolved Spectroscopy: Instrumentation and Applications* (pp. 1–55). <https://doi.org/10.1002/9780470027318.a9555>

[26] Zha, J., & Roggendorf, H. (1991). Sol–gel science, the physics and chemistry of sol–gel processing, Ed. by C. J. Brinker and G. W. Scherer, Academic Press, Boston 1990, xiv, 908 pp., bound—ISBN 0-12-134970-5. *Advanced Materials*, 3(10), 522.

<https://doi.org/https://doi.org/10.1002/adma.19910031025>

[27] Kianfar, E., & Suksatan, W. (2021). Nanomaterial by Sol-Gel Method: Synthesis and Application. *Advances in Materials Science and Engineering*, 2021, 1–21.

<https://doi.org/10.1155/2021/5102014>

[28] Singh, V., Kaur, S., Rao, A. S., Rao, J. L., & Irfan, M. (2020). PL and EPR characteristics of Gd³⁺-activated SrMgSi₂O₆ phosphor prepared by sol-gel procedure.

Optik, 204, 164157. <https://doi.org/https://doi.org/10.1016/j.ijleo.2019.164157>

[29] Singh, V., Yadav, A., Annapurna Devi, Ch. B., Rao, A. S., & Singh, N. (2021). Luminescence properties of Sm³⁺ doped LaP₃O₉ phosphors. *Optik*, 242, 167264.

<https://doi.org/https://doi.org/10.1016/j.ijleo.2021.167264>

[30] Singh, V., Kaur, S., & Rao, A. S. (2021). Visible luminescence in Sm³⁺ doped CaY₂Al₄SiO₁₂ garnet obtained by sol-gel method. *Optik*, 245, 167394.

<https://doi.org/https://doi.org/10.1016/j.ijleo.2021.167394>

[31] Balakrishna, A., Swart, H. C., Ramaraghavulu, R., Bedyal, A. K., Kroon, R. E., & Ntwaeaborwa, O. M. (2017). Structural evolution induced by substitution of designated molybdate sites (MoO₄²⁻) with different anionic groups (BO₃³⁻, PO₄³⁻ and SO₄²⁻) in CaMoO₄:Sm³⁺ phosphors—A study on color tunable luminescent properties. *Journal of Alloys and Compounds*, 727, 224–237.

<https://doi.org/https://doi.org/10.1016/j.jallcom.2017.08.117>

[32] Kumar, S., Khajuria, P., Mahajan, R., Sharma, V. D., Lee, Y., & Prakash, R. (2020). Synthesis and spectral properties of Sm³⁺ doped MgAl₂O₄ phosphor. *AIP Conference Proceedings*, 2220(1), 020011. <https://doi.org/10.1063/5.0001443>

- [33] Shrivastava, R., & Kaur, J. (2015). Characterisation and Mechanoluminescence studies of Sr₂MgSi₂O₇: Eu²⁺, Dy³⁺. *Journal of Radiation Research and Applied Sciences*, 8(2), 201–207. <https://doi.org/https://doi.org/10.1016/j.jrras.2015.01.005>
- [34] Sahu, I. P., Bisen, D. P., Brahme, N., & Tamrakar, R. K. (2015). Photoluminescence properties of europium doped di-strontium magnesium di-silicate phosphor by solid state reaction method. *Journal of Radiation Research and Applied Sciences*, 8(1), 104–109. <https://doi.org/https://doi.org/10.1016/j.jrras.2014.12.006>
- [35] Annadurai, G., Kennedy, S. M. M., & Sivakumar, V. (2016). Photoluminescence properties of a novel orange-red emitting Ba₂CaZn₂Si₆O₁₇:Sm³⁺ phosphor. *Journal of Rare Earths*, 34(6), 576–582. [https://doi.org/https://doi.org/10.1016/S1002-0721\(16\)60064-9](https://doi.org/https://doi.org/10.1016/S1002-0721(16)60064-9)
- [36] Tu, D., Liang, Y., Liu, R., Cheng, Z., Yang, F., & Yang, W. (2011). Photoluminescent properties of LiSrxBal-xPO₄:RE³⁺ (RE=Sm³⁺, Eu³⁺) f-f transition phosphors. *Journal of Alloys and Compounds*, 509(18), 5596–5599. <https://doi.org/https://doi.org/10.1016/j.jallcom.2011.02.077>
- [37] Kaur, S., Katyal, V., Plakkot, V., Deopa, N., Prasad, A., & Rao, A. S. (2021). Radiative emission analysis of Sm³⁺ ions doped borosilicate glasses for visible orange photonic devices. *Journal of Non-Crystalline Solids*, 572, 121106. <https://doi.org/https://doi.org/10.1016/j.jnoncrysol.2021.121106>
- [38] Annadurai, G., Kennedy, S. M. M., & Sivakumar, V. (2016). Photoluminescence properties of a novel orange-red emitting Ba₂CaZn₂Si₆O₁₇:Sm³⁺ phosphor. *Journal of Rare Earths*, 34(6), 576–582. [https://doi.org/https://doi.org/10.1016/S1002-0721\(16\)60064-9](https://doi.org/https://doi.org/10.1016/S1002-0721(16)60064-9)

- [39] Singh, V., Kaur, S., & Rao, A. S. (2021). Visible luminescence in Sm³⁺ doped CaY₂Al₄SiO₁₂ garnet obtained by sol-gel method. *Optik*, 245, 167394. <https://doi.org/https://doi.org/10.1016/j.ijleo.2021.167394>
- [40] Sun, J., & Cui, D. (2014). Synthesis, Structure, and Thermally Stable Luminescence of Dy³⁺-Doped Na₃YSi₂O₇ Host Compound. *Journal of the American Ceramic Society*, 97(3), 843–847. <https://doi.org/https://doi.org/10.1111/jace.12703>
- [41] Xu, D., Yang, Z., Sun, J., Gao, X., & Du, J. (2016). Synthesis and luminescence properties of double-perovskite white emitting phosphor Ca₃WO₆:Dy³⁺. *Journal of Materials Science: Materials in Electronics*, 27(8), 8370–8377. <https://doi.org/10.1007/s10854-016-4848-z>

PLAGIARISM REPORT



Similarity Report ID: oid:27535:36507003

PAPER NAME

Copy of Final Dissertation Report 2.pdf

WORD COUNT

8933 Words

CHARACTER COUNT

51529 Characters

PAGE COUNT

38 Pages

FILE SIZE

222.7KB

SUBMISSION DATE

May 30, 2023 3:11 PM GMT+5:30

REPORT DATE

May 30, 2023 3:12 PM GMT+5:30

● 3% Overall Similarity

The combined total of all matches, including overlapping sources, for each database.

- 1% Internet database
- 1% Publications database
- Crossref database
- Crossref Posted Content database
- 1% Submitted Works database

● Excluded from Similarity Report

- Bibliographic material
- Quoted material
- Cited material
- Small Matches (Less than 14 words)

Abstract acceptance mail

5/30/23, 8:15 PM

Delhi Technological University Mail - ICTN-KLC 2023- Poster Presentation



Rajat Katiyar 2K21/MSCPHY/61 <rajatkatiyar_2k21mscphy61@dtu.ac.in>

ICTN-KLC 2023- Poster Presentation

1 message

ICTN-KLC 2023 <tfl.conf@gmail.com>

Sun, May 28, 2023 at 1:10 PM

To: Somnath Chanda Roy <somnath@iitm.ac.in>, Sanjur <sanjur@srmist.edu.in>

Bcc: rajatkatiyar_2k21mscphy61@dtu.ac.in

Dear Participant,

We are happy to receive your abstract for the presentation in ICTN-KLC 2023 and pleased to let you know that it has been selected for **Poster Presentation**. The abstract number can be found on the home page under the link "**list of selected abstracts**" on the conference website (ICTN-KLC 2023). Please note that

- 1- The registration fee payment link will remain active till May 31, 2023.
- 2- The poster template will be shared on the conference website soon.

Feel free to get in touch with us (through email to tfl.conf@gmail.com) if you have any questions or concerns.

Looking forward to seeing you at the IIT Madras campus during July 6-8, 2023.

Best Wishes

Organising Committee (ICTN-KLC-2023)

REGISTRATION PROOF

International Conference on Thin Films and Nanotechnology - Knowledge, Leadership and Commercialization (ICTN-KLC) 2023 **X**

Name	Rajat Katiyar
Email id	naman.katiyar56@gmail.com
Mobile	+919911317058
Abstract Title	Optical and structural studies of samarium doped strontium magneto silicate phosphor synthesised via sol-gel.
Abstract No	G-021
Category	Student with accommodation
Organization	Delhi Technological University
Department	Applied Physics
City	Delhi
Country	India
Payment id	Pay-Lvu4d53WZvH70D
Payment status	complete
Paid amount	INR: 7000

PROOF OF SCOPUS INDEXING

03/02/23, 8:35 PM

Journal of Materials Science: Materials in Electronics | Home



Search Authors & Editors Log in



Journal of Materials Science: Materials in Electronics

[Editorial board](#) [Aims & scope](#) [Journal updates](#)

The Journal of Materials Science: Materials in Electronics is an established refereed companion to the Journal of Materials Science. It publishes papers on materials and their applications in modern electronics, covering the ground between fundamental science, such as semiconductor physics, and work concerned specifically with applications. It explores the growth and preparation of new materials, as well as their processing, fabrication, bonding and encapsulation, together with the reliability, failure analysis, quality assurance and characterization related to the whole range of applications in electronics. The Journal presents papers in newly developing fields such as low dimensional structures and devices, optoelectronics including III-V compounds, glasses and linear/non-linear crystal materials and lasers, high Tc superconductors, conducting polymers, thick film materials and new contact technologies, as well as the established electronics device and circuit materials.

[Show all](#)

Editor-in-Chief

Safa O. Kasap

Publishing model

Hybrid (Transformative Journal). [How to publish with us, including Open Access](#)

2.779 (2021)

Impact factor

2.401 (2021)

Five year impact factor

23 days

Submission to first decision (Median)

1,368,227 (2021)

Downloads

For authors

[Submission guidelines](#)

[Language editing services](#)

[Ethics & disclosures](#)

[Open Access fees and funding](#)

[Contact the Journal](#)

Submit manuscript



Working on a manuscript?

Avoid the most common mistakes and prepare your manuscript for journal editors.

[Learn more](#) →

Explore

[Volumes and issues](#)

[Collections](#)

Sign up for alerts

Latest issue



Volume 34
Issue 15, May 2023

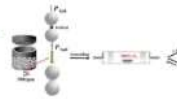
[View all volumes and issues](#) >

Latest articles

[Flaky FeSiAl powders with high permeability towards broadband microwave absorption through tuning aspect ratio](#)

Zhi Cao, Wei Liu ... Xuebin Zheng

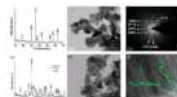
OriginalPaper | Published: 30 May 2023 | Article: 1249



[Phase components, microstructures, and magnetic properties of liquid-phase-sintered \$\text{Li}_{0.4}\text{Zn}_{0.2}\text{Fe}_{2.4}\text{O}_4/\text{Y}_3\text{Fe}_5\text{O}_{12}\$ ferrite nanocomposites](#)

Yixing Gao, Lichuan Jin ... Tingchuan Zhou

OriginalPaper | Published: 30 May 2023 | Article: 1250



[Magneto-dielectric properties of \$\text{Ni}_{0.95}\text{Cu}_{0.05}\text{Zn}_{0.50}\text{Fe}_2\text{O}_4\text{-BaTiO}_3\$ and its application as substrate of microstrip patch antennas](#)

F. H. Ikhsan, S. K. Yee ... Adel Y. I. Ashyap



<https://www.springer.com/journal/10954/>

1/1

OriginalPaper | Published: 30 May 2023 | Article: 1251

[Effect of yttrium on the structural, dielectric, and magnetic properties of Co-doped ZnO magnetic nanorods for potential spintronic applications](#)


Aziz Ullah, Inam Ullah Khan ... Rajwali Khan

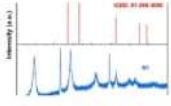
OriginalPaper | Published: 30 May 2023 | Article: 1252


[Hydrothermal synthesis of nickel oxide nanoflowers as a blend of 1D and 2D morphologies for its improved OER activity and supercapacitance](#)

Sanjay Upadhyay, Niraj Kumar ... O. P. Pandey

OriginalPaper | Published: 30 May 2023 | Article: 1253





 This journal has [271 open access articles](#)

[View all articles >](#)

About this journal

Electronic ISSN 1573-482X
Print ISSN 0957-4522

Abstracted and indexed in

BFI List
Baidu
CLOCKSS
CNKI
CNPIEC
Chemical Abstracts Service (CAS)
Current Contents Collections / Electronics & Telecommunications Collection
Current Contents/Engineering, Computing and Technology
Current Contents/Physical, Chemical and Earth Sciences
Dimensions
EBSCO Applied Science & Technology Source
EBSCO Computers & Applied Sciences Complete
EBSCO Discovery Service
EBSCO Engineering Source
EBSCO OmniFile
EBSCO STM Source
EBSCO Science Full Text Select
EI Compendex
Google Scholar
INIS Atomindex
INSPEC
Japanese Science and Technology Agency (JST)
Journal Citation Reports/Science Edition
Naver
OCLC WorldCat Discovery Service
Portico
ProQuest Abstracts in New Technologies and Engineering (ANTE)
ProQuest Advanced Technologies & Aerospace Database
ProQuest-ExLibris Primo
ProQuest-ExLibris Summon
SCImago
SCOPUS
Science Citation Index
Science Citation Index Expanded (SCIE)
Semantic Scholar
TD Net Discovery Service
UGC-CARE List (India)
Wanfang

Copyright information

[Rights and permissions](#)
[Springer policies](#)

© Springer Science+Business Media, LLC, part of Springer Nature